THEORETICAL DEVELOPMENT AND IMPLEMENTATION OF ALGORITHMS FOR THE INVERSION OF FREQUENCY DOMAIN AIRBORNE ELECTROMAGNETIC DATA INTO A LAYERED EARTH

Jacobus Petrus Smit

Submitted in partial fulfillment of the requirements for the degree Magister Scientiae

In the Faculty of Natural and Agricultural Sciences, School of Physical Sciences, Department of Geology

University of Pretoria

October 2005

Summary

Equations for determining the electromagnetic response for a dipole situated above a layered earth are derived from Maxwell's equations. The theory is then expanded to allow for a transmitter and receiver at any distance above the surface of the layered earth. Using the commercially available software "Mathcad" standard curves are calculated for two- and three layer models.

Damped least squares inversion is advocated. The partial derivatives of the layered earth expression with respect to all model parameters are formulated and the Jacobian matrix is constructed. The inversion routine is tested on noise-free synthetic data and on synthetic data with noise.

The study is concluded with a case history where the developed technology is applied to a DIGHEM V data set flown over the Nebo granites in the Ga-Masemola area, Limpopo Province, South Africa. Results show that although the data consists of only three co-planar frequencies, parameters such as depth to bedrock, overburden conductivity and bedrock conductivity can be recovered.

Acknowledgements

I wish to express my gratitude to the Council for Geoscience for granting me a statutory project (Project number 2003-0840) with the title "Algorithms for the interpretation of airborne EM data". Most results obtained in developing these algorithms have been used in this thesis.

I wish to thank my friend and co-supervisor Prof. Dr. E.H. Stettler for his continuous support and guidance. I also wish to express gratitude to Prof. Felix Kamenetsky (Maximillian University, Munich) for meaningful discussions and Dr. V. Zadorozhnaya (Council for Geoscience) for her contribution. Many thanks to Magdel Combrinck for all her constructive comments and suggestions.

Lastly I would like to express my gratitude to the Council for Geoscience, Fugro Airborne Surveys and The University of Pretoria for having access to the Nebo granite DIGHEM V data set.

SYMBOLS AND NOTATION

E Electric field intensity (V/m)

B Magnetic induction (T)

H Magnetic field intensity (A/m)

J Electric current density (A/m^2)

D Electric displacement (C/m^2)

M Magnetic dipole moment ($A \cdot m^2$)

A, Π, F vector potentials.

σ conductivity (S/m)

ε dielectric constant (F/m)

ε_0 permittivity of free space

μ magnetic susceptibility (H/m)

μ_0 magnetic susceptibility of free space

μ_n magnetic susceptibility of the n^{th} layer divided by μ_0

ω angular frequency $(2\pi f)$

f frequency (Hz)

ς charge density (C/m^3)

k wavenumber

δ skindepth (m)

ρ dipole separation (m)

λ integration variable

$i = \sqrt{-1}$

CONTENTS *Page Number*

List of Figures

Page Number

1. MOTIVATION

Numerous imaging methods for airborne electromagnetic data exist. Due to the large amount of data acquired during a normal day's surveying (typically 4 million soundings which are stacked and averaged to between 50 000 and 100 000 individual soundings) any imaging algorithm has to be very fast and needs to recover as much as possible subsurface information present in the data.

Fast approximate inversion of FDEM data was first proposed by Sengpiel (1988) and later refined by Huang and Fraser (1996) and Sengpiel and Siemon (2000). The method yields for every frequency an apparent depth or "centroid" depth and an apparent resistivity. If the data consists of many frequencies the method enables a fast approximation of the subsurface conductivity distribution.

One of the most popular imaging algorithms called the Conductivity-Depth Transform (Macnae and Lamontagne, 1987; Macnae et al., 1991; Stolz and Macnae, 1998) is used by airborne contractors as part of a standard interpretation of time domain electromagnetic data (TDEM). The method finds the depth to an equivalent current filament as a function of time, from which the diffusion velocity and hence the conductivity can be determined. Due to heavy smoothing of data before processing, coupled data are not identified and lateral smoothing smears out the distortions of the coupled data to the uncoupled data sets (Christiansen and Christensen, 2003). An imaging method employed by the Russians called the S_τ version transforms TDEM data to apparent conductivity (Sidorov and Tikshaev, 1970). By

making use of profile plots these apparent conductivity curves provides a fast way of delineating good conductors. Other imaging methods have, amongst others, been proposed by Christensen (2002), Smith et al. (1994) and Polzer (1985).

The subject of this thesis is the development of a theoretical base for the damped least squares inversion of airborne electromagnetic data to a one dimensional layered earth. This is done for a generic airborne platform typically used for time domain systems where the transmitter is fixed on the aircraft perimeter and the receiver is pulled behind and below the aircraft in a 'bird' (Figure 2.1). This geometry however can also be used for frequency domain systems as demonstrated by the Russian company Aerogeofisika based in Moscow.

The methodology that is adopted is to apply the inversion routine in the frequency domain. The theory is therefore developed in the frequency domain. Normally, frequency domain inversion algorithms assume co-planar geometry since this approximation simplifies the mathematical description (Haung and Fraser, 2003). The approach followed here however implies that any transmitter / receiver geometry can be accommodated with no loss of generality. The advantage of this approach is that TDEM data converted to the frequency domain can also be processed with the developed algorithms.

The electromagnetic equations for a vertical magnetic dipole situated above a horizontally layered earth are developed from Maxwell's equations following the classical approach of Keller and Frischknecht (1966) and Kaufman and Keller (1983). The aim of this thesis is the development of a

fast semi-automatic inversion routine for the interpretation of airborne electromagnetic data. The shortcomings of the derived expressions for implementation into a computer program are discussed. The electromagnetic equations for a vertical magnetic dipole situated above a horizontally layered earth published by Ward and Hohmann (1988) are subsequently incorporated in the inversion algorithm.

Algorithms are then developed for the inversion of field data to either a halfspace, a two layered or a three layered conductive earth. The robustness of the technique is proven on synthetic and real data. Currently the quality and design parameters of frequency domain airborne data do not lend itself to obtaining layer parameters beyond three layers.

2. BASIC PRINCIPLES

2.1 MAXWELL'S EQUATIONS

Maxwell's equations, one of the corner stones of physics, describe the relationship between various electric fields, magnetic fields and medium parameters. In differential form they are as follows:

$$\nabla \times \mathbf{E} = \frac{-\partial \mathbf{B}}{\partial t} \tag{2.1}$$

$$\nabla \times \mathbf{H} = \mathbf{J} + \frac{\partial \mathbf{D}}{\partial t} \tag{2.2}$$

$$\nabla \cdot \mathbf{E} = \frac{-\varsigma}{\varepsilon_0} \tag{2.3}$$

$$\nabla \cdot \mathbf{B} = 0 \tag{2.4}$$

with,

E = electric field intensity in Volt/meter (V/m)

B = magnetic induction in Tesla (T)

D = dielectric displacement in Coulomb/m^2 (C/m^2)

H = magnetic field intensity in Ampere-turn/m (A/m)

ς = charge density in Coulomb/ m^3 (C/m^3)

ε_0 = dielectric permittivity of free space

To enable the analyses of electromagnetic induction, certain assumptions have to be made to simplify the study. In this discussion it is assumed that the subsurface is linear, isotropic and homogeneous. Those assumptions allow us to use the following constitutive equations:

$$\mathbf{J} = \sigma \mathbf{E} \tag{2.5}$$

$$\mathbf{D} = \varepsilon\mathbf{E} \tag{2.6}$$

$$\mathbf{B} = \mu\mathbf{H} \tag{2.7}$$

with,

σ = conductivity in Siemens/m (S/m)

ε = dielectric constant in Farad/m (F/m)

μ = magnetic susceptibility in Henry/m (H/m)

J = current density in Ampére/ m^2 (A/m^2)

If we further assume that there is no free electric charge or current in the medium, Maxwell's equations, for a periodic time dependence, becomes:

$$\nabla \times \mathbf{E} = i\omega\mu\mathbf{H} \tag{2.8}$$

$$\nabla \times \mathbf{H} = \sigma\mathbf{E} - i\omega\varepsilon\mathbf{E} \tag{2.9}$$

$$\nabla \cdot \mathbf{E} = 0 \tag{2.10}$$

$$\nabla \cdot \mathbf{H} = 0 \tag{2.11}$$

where,

$\omega = 2\pi f$ (angular frequency)

f = frequency in Hertz (Hz)

$i = \sqrt{-1}$

The following assumptions have been made in reducing Maxwell's equations:

1. ς = 0. Charge density inside a uniform halfspace is zero.
2. $\sigma \neq 0$. The resistivity inside a uniform halfspace is finite.
3. $\frac{\partial \mathbf{D}}{\partial t} << \mathbf{J}$ for a quasi-stationary field.

4. We assume a harmonic time varying field $\Rightarrow \mathbf{E}, \mathbf{H} \propto e^{-i\omega t}$ with $e^{-i\omega t} = \cos\omega t - i\sin\omega t$. Therefore, $\mathbf{E} = \mathbf{E}_0 e^{-i\omega t}$ and $\mathbf{B} = \mathbf{B}_0 e^{-i\omega t}$

Following the quasi-static approximation equation (2.9) becomes:

$$\nabla \times \mathbf{H} = \sigma \mathbf{E} \tag{2.12}$$

2.2. WAVENUMBER AND SKIN DEPTH

From equations (2.8) and (2.9) we can write:

$$\nabla \times \nabla \times \mathbf{E} = i\mu\omega(\nabla \times \mathbf{H})$$

$$= i\mu\omega(\sigma\mathbf{E} - i\varepsilon\omega\mathbf{E}) \tag{2.13}$$

By making use of vector identities, equation (2.13) can be written as:

$$\nabla(\nabla \cdot \mathbf{E}) - \nabla^2\mathbf{E} = i\mu\omega(\sigma\mathbf{E} - i\varepsilon\omega\mathbf{E}) \tag{2.14}$$

In the quasi-static approximation $\nabla \cdot \mathbf{E} = 0$ and $\nabla \cdot \mathbf{H} = 0$. From equation (2.14) we have:

$$\nabla^2\mathbf{E} = -\mathbf{E}(i\mu\omega\sigma + \mu\varepsilon\omega^2) \tag{2.15}$$

Therefore

$$(\nabla^2 + k^2)\mathbf{E} = 0 \tag{2.16}$$

where k is called the wavenumber and is given by:

$$k^2 = \omega\mu(i\sigma + \varepsilon\omega) \tag{2.17}$$

At low induction numbers the square of k is given by:

$$k^2 = i\omega\mu\sigma \tag{2.18}$$

Equation (2.16) contains all the information that can be determined from the subsurface. If one takes the complex root of equation (2.18) you have

$$k = \frac{1}{\delta} + i\frac{1}{\delta}$$

where $\delta = \sqrt{\frac{2}{\omega\mu\sigma}}$ (Telford et al., 1990). (2.19)

δ is called the skin depth and provides the depth limit at which meaningful information can be obtained. It is also defined as the distance in the halfspace that a propagating plane wave has travelled when its amplitude has been attenuated to $\frac{1}{e}$ of its value at surface (Kaufmann and Keller, 1983).

2.3. THE WAVE EQUATION

According to Faraday:

$$\nabla \times \mathbf{E} = i\omega\mu\mathbf{H} \quad (2.20)$$

If

$$\mathbf{H} = \nabla \times \mathbf{A}$$

then

$$\nabla \times \mathbf{E} = i\omega\mu(\nabla \times \mathbf{A}) \quad (2.21)$$

$\mathbf{A}$ is a vector potential and is introduced to simplify the solution. It is based on the fact that $\nabla \cdot \mathbf{H} = 0$ (Kaufmann and Keller (1983) p.217).

$$\nabla \times (\mathbf{E} - i\omega\mu\mathbf{A}) = 0 \quad (2.22)$$

Therefore

$$\mathbf{E} = i\omega\mu\mathbf{A} - \nabla U \quad (2.23)$$

where U is a scalar potential that has been defined arbitrarily.

If we replace **H** and **E** now in equation (2.12) we have

$$\nabla \times \nabla \times \mathbf{A} = i\omega\mu\sigma\mathbf{A} - \sigma\nabla U \tag{2.24}$$

Using the vector identity:

$$\nabla \times \nabla \times \mathbf{A} = \nabla(\nabla \cdot \mathbf{A}) - \nabla^2\mathbf{A} \tag{2.25}$$

we can rewrite equation (2.24)

$$\nabla(\nabla \cdot \mathbf{A}) - \nabla^2\mathbf{A} = i\omega\mu\sigma\mathbf{A} - \sigma\nabla U \tag{2.26}$$

By defining the gauge condition

$$-\sigma U = \nabla \cdot \mathbf{A} \text{ (Kaufmann and Keller (1983) p. 218)} \tag{2.27}$$

we can calibrate equation (2.26) to eliminate further consideration of the scalar potential U. We then have

$$-\sigma\nabla U - \nabla^2\mathbf{A} = k^2\mathbf{A} - \sigma\nabla U \tag{2.28}$$

and

$$\nabla^2\mathbf{A} + k^2\mathbf{A} = 0 \tag{2.29}$$

Equation (2.29) is known as the wave equation for the vector potential $\mathbf{A}$.

In the same way as in equation (2.21) we can define a vector potential $\mathbf{\Pi}$ based on the fact that $\nabla \cdot \mathbf{E} = 0$ (Kaufmann and Keller (1983) p. 26)

$$\mathbf{E} = i\omega\mu(\nabla \times \mathbf{\Pi}) \tag{2.30}$$

Once again, by substitution into equation (2.12) we get

$$\nabla \times \mathbf{H} = i\omega\mu\sigma(\nabla \times \mathbf{\Pi})$$

$$\nabla \times (\mathbf{H} - i\omega\mu\sigma\mathbf{\Pi}) = 0$$

and

$$\mathbf{H} = i\omega\mu\sigma\mathbf{\Pi} - \nabla U$$

where U is a scalar potential that has been defined arbitrarily.

Substitution into equation (2.8) gives

$$i\omega\mu(\nabla \times \nabla \times \mathbf{\Pi}) = i\omega\mu(i\omega\mu\sigma\mathbf{\Pi} - \nabla U)$$

and utilizing the vector identity (equation (2.25)) we obtain

$$\nabla(\nabla \cdot \mathbf{\Pi}) - \nabla^2\mathbf{\Pi} = i\omega\mu\sigma\mathbf{\Pi} - \nabla U$$

If we now define the gauge condition as:

$$U = -\nabla \cdot \mathbf{\Pi}$$

we can write the wave equation in terms of the vector potential $\mathbf{\Pi}$

$$\nabla^2\mathbf{\Pi} + k^2\mathbf{\Pi} = 0 \qquad (2.31)$$

and we can rewrite Maxwell's electromagnetic field equations as:

$$\mathbf{E} = i\omega\mu(\nabla \times \mathbf{\Pi})$$

and

$$\mathbf{H} = k^2\mathbf{\Pi} + \nabla(\nabla \cdot \mathbf{\Pi}) \qquad (2.32)$$

If we assume a vertical magnetic dipole then the symmetry of the electromagnetic field implies that $\mathbf{E}$ only has a tangential component, $\mathbf{\Pi}$ only has a z (vertical) component and $\mathbf{H}$ a z (vertical) and radial component. By using cylindrical vector derivatives we have:

$$\mathbf{E}_\phi = -i\omega\mu\frac{\partial\mathbf{\Pi}_z}{\partial r} \qquad (2.33)$$

$$\mathbf{H}_z = k^2\mathbf{\Pi}_z + \frac{\partial^2\mathbf{\Pi}_z}{\partial z^2} \qquad (2.34)$$

and

$$\mathbf{H}_r = \frac{\partial^2 \mathbf{\Pi}_z}{\partial r \partial z} \tag{2.35}$$

Using the boundary conditions from electromagnetic theory we know that the tangential components of the electric and magnetic fields have to be continuous across an interface (between medium 1 and medium 2 for example (Figure 2.1)), hence from equation (2.35):

$$\frac{\partial^2 \mathbf{\Pi}_{1z}}{\partial r \partial z} = \frac{\partial^2 \mathbf{\Pi}_{2z}}{\partial r \partial z} \tag{2.36}$$

and from equation (2.33)

$$\frac{\partial \mathbf{\Pi}_{1z}}{\partial r} = \frac{\partial \mathbf{\Pi}_{2z}}{\partial r} \tag{2.37}$$

The tangential components of the electromagnetic field are continuous across the interface if the vector potential $\mathbf{\Pi}_z$ and its vertical derivative are continuous.

With reference to Figure 2.1 we consider the air, conducting halfspace interface. At the surface we have $z = -H$. The z axis points positive upwards with the origin at the transmitter. The solution for the vector potential in the upper halfspace, i.e. for the magnetic dipole situated above the surface, can be written as:

$$\mathbf{\Pi}_{1z} = \mathbf{\Pi}_{0z} + \mathbf{\Pi}_{2z} \tag{2.38}$$

where $\mathbf{\Pi}_{0z}$ is the vector potential for a magnetic dipole in an empty full-space and $\mathbf{\Pi}_{2z}$ is the vector potential contributed from the conducting halfspace.

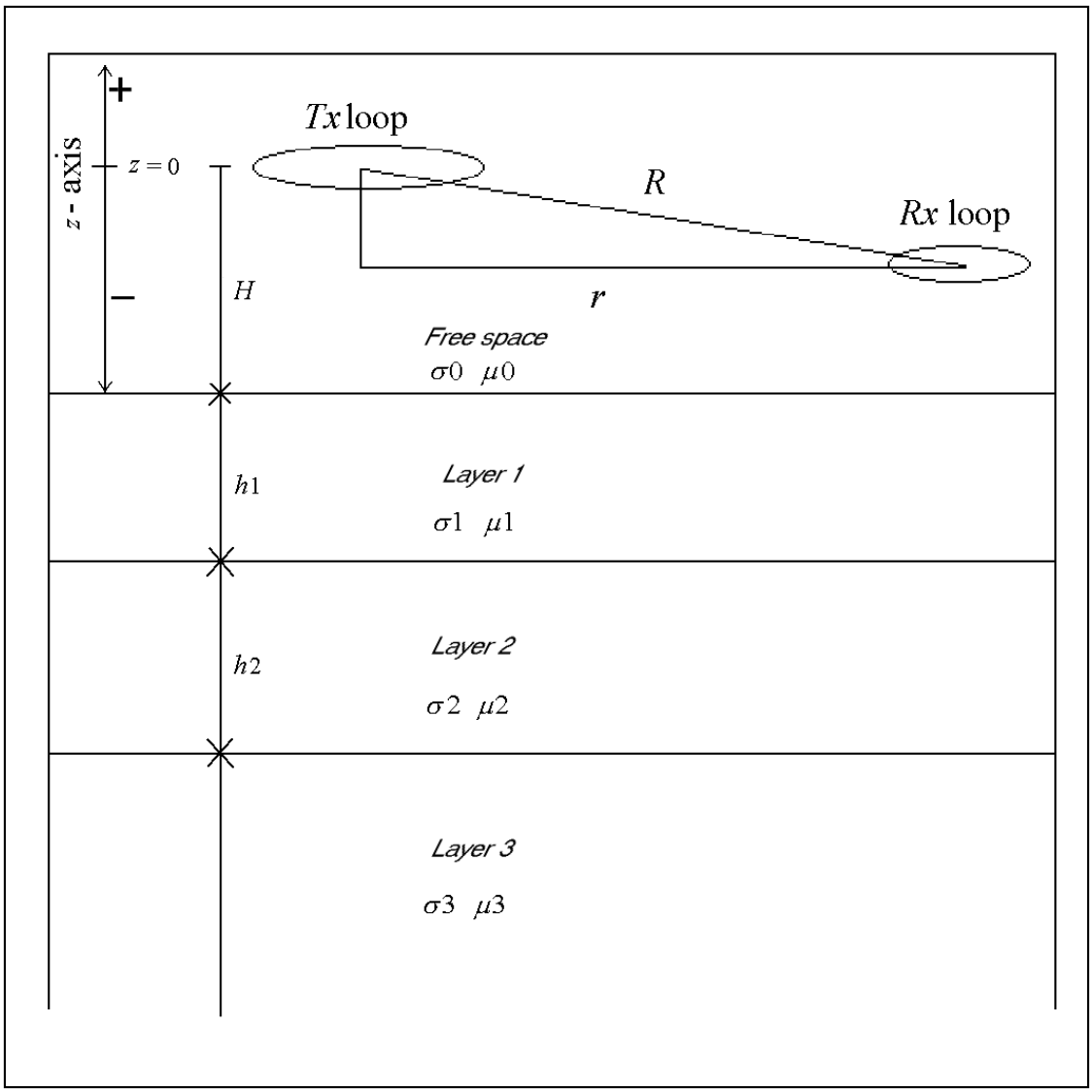

Figure 2.1. Airborne EM system configuration above a 3-layered conductive earth.

The vector potential in full-space can be written as:

$$\mathbf{\Pi}_{0z} = \frac{\mathbf{M}}{4\pi}\frac{1}{R} \tag{2.39}$$

where $R = \left(r^2 + z^2\right)^{\frac{1}{2}}$ and **M** is the magnetic dipole moment with **M** = $qIA\hat{a}$

where,

q is the amount of turns in the loop

$I = I_0\, e^{-i\omega t}$ and is the alternating current flowing in the loop

A is the surface area of the loop in (m^2) and

$\hat{a}$ is a unit vector perpendicular to the surface area

In order to apply the boundary conditions we must find a solution to the following equations.

$$\nabla^2\mathbf{\Pi}_{1z} = 0 \quad \text{if z > -}H \tag{2.40}$$

above the surface of the conducting halfspace ($k^2 = 0$ in the air)

and

$$\nabla^2\mathbf{\Pi}_{2z} + k^2\mathbf{\Pi}_{2z} = 0 \text{ if z < -}H \tag{2.41}$$

below the surface of the conducting halfspace

If we expand (2.41) in cylindrical coordinates and discard the term where differentiation with respect to ϕ takes place (due to the cylindrical symmetry), differentiation in parts give,

$$\frac{\partial^2\mathbf{\Pi}_z(r,z)}{\partial r^2} + \frac{1}{r}\cdot\frac{\partial\mathbf{\Pi}_z(r,z)}{\partial r} + \frac{\partial^2\mathbf{\Pi}_z(r,z)}{\partial z^2} + k^2\mathbf{\Pi}_z = 0 \tag{2.42}$$

If we apply separation of variables we can write (2.42) as the product of two functions with each function only dependant on one variable.

$$\mathbf{\Pi}_z = U(r)V(z) \tag{2.43}$$

Equation (2.42) can now be written as

$$V(z)\cdot\frac{d^2U(r)}{dr^2}+V(z)\cdot\frac{1}{r}\cdot\frac{dU(r)}{dr}+U(r)\cdot\frac{d^2V(z)}{dz^2}+k^2U(r)V(z)=0 \tag{2.44}$$

Dividing (2.44) with *U(r)V(z)* yields

$$\frac{1}{U}\cdot\frac{d^2U}{dr^2}+\frac{1}{Ur}\cdot\frac{dU}{dr}+\frac{1}{V}\frac{d^2V}{dz^2}+k^2=0 \tag{2.45}$$

Equation (2.45) can now be written as

$$\frac{1}{U}\cdot\frac{d^2U}{dr^2}+\frac{1}{Ur}\cdot\frac{dU}{dr}=-\left(\frac{1}{V}\frac{d^2V}{dz^2}+k^2\right) \tag{2.46}$$

Since U and V are independent, each side of equation (2.46) must be equal to a constant. Hence we can write two ordinary differential equations instead of the partial differential equation of (2.42)

$$\frac{1}{U}\cdot\frac{d^2U}{dr^2}+\frac{1}{Ur}\cdot\frac{dU}{dr}=\lambda^2 \tag{2.47}$$

$$\frac{1}{V}\cdot\frac{d^2V}{dz^2}+k^2=-\lambda^2 \tag{2.48}$$

where λ is a separation constant. Equations (2.47) and (2.48) can now be written as

$$\frac{d^2U}{dr^2} + \frac{1}{r} \cdot \frac{dU}{dr} - \lambda^2 U = 0 \tag{2.49}$$

$$\frac{d^2V}{dz^2} - (-\lambda^2 - k^2)V = 0 \tag{2.50}$$

Solutions for equation (2.49) are Bessel functions of the first and second kind. The Bessel function of the second kind $Y_0(\lambda r)$ has the property of being infinite along the z axis when $r = 0$. This does not describe the field behaviour for a point source adaquately. We can however write a solution for equation (2.50) where

$$V = C_\lambda e^{\left(\lambda^2 + k^2\right)^{1/2} z} + D_\lambda e^{-\left(\lambda^2 + k^2\right)^{1/2} z} \tag{2.51}$$

A general solution for equation (2.42) can now be given for all possible values of λ in the form of a Hankel transform integral

$$\mathbf{\Pi}_z = \frac{M}{4\pi} \int_0^\infty \left(D_\lambda e^{-\lambda_1 z} + C_\lambda e^{\lambda_1 z} \right) J_0(\lambda r) d\lambda \tag{2.52}$$

where D_λ and C_λ are unknown coefficients, $\lambda_1 = (\lambda^2 + k_1^2)^{1/2}$ and $k_1^2 = i\omega\mu\sigma_1$ where σ_1 is the conductivity of the conductive halfspace.

Because the electromagnetic field decreases with distance from source we can omit the second term from equation (2.51) for the dipole in a conductive halfspace and write

$$\mathbf{\Pi}_{2z} = \frac{M}{4\pi}\int_0^{\infty} C_\lambda e^{\lambda_1 z} J_0(\lambda r) d\lambda \quad \text{for } z < -H \tag{2.53}$$

In free space on the other hand $k = 0$, therefore $\lambda_1 = \lambda$ and with $z > 0$ we have, from equations (2.38) and (2.39)

$$\mathbf{\Pi}_{1z} = \frac{M}{4\pi}\left[\frac{1}{R} + \int_0^{\infty}\left(D_\lambda e^{-\lambda z}\right) J_0(\lambda r) d\lambda\right] \text{for } z > 0 \tag{2.54}$$

2.4. THE FREQUENCY DOMAIN RESPONSE FOR A ONE, TWO AND THREE LAYERED EARTH MODEL

For convenience lets define the vector potential for a magnetic dipole as

$$\mathbf{F} = i\mu\omega\mathbf{\Pi}. \tag{2.55}$$

The primary vector potential **F** for a magnetic dipole is given by:

$$\mathbf{F} = \frac{i\omega\mu\mathbf{M}}{4\pi R} e^{-kR} \text{ (Keller and Frischknecht (1966) p. 331)} \tag{2.56}$$

The potential functions for all five regions must be a solution to the wave equation

$$\nabla^2\mathbf{F} + k^2\mathbf{F} = 0 \tag{2.57}$$

which implies we have to solve equation (2.42) for the magnetic vector potential functions in all the regions (i.e. above the transmitter, below the transmitter and in the first, second and third layer). Following Keller and Frischknecht (1966) we can write the vector potential functions in the five different regions by making use of equations (2.52 – 2.56).

$$\mathbf{F}_1 = C\left[\frac{e^{-k_0 R}}{R} + \int_0^\infty \psi_1(\lambda) e^{(-\lambda_0 z)} J_0(\lambda r) d\lambda\right] \text{ for } z > 0 \tag{2.58}$$

$$\mathbf{F}_2 = C\left[\frac{e^{-k_0 R}}{R} + \int_0^\infty [\psi_2(\lambda) e^{(-\lambda_0 z)}] J_0(\lambda r) d\lambda\right] \text{ for } -H < z < 0 \tag{2.59}$$

$$\mathbf{F}_3 = C\left[\int_0^\infty [\psi_3(\lambda) e^{(\lambda_1 z)} + \psi_4(\lambda) e^{(-\lambda_1 z)}] J_0(\lambda r) d\lambda\right]$$

for $-(H+h_1) < z < -H$ (2.60)

$$\mathbf{F}_4 = C\left[\int_0^\infty [\psi_5(\lambda) e^{(\lambda_2 z)} + \psi_6(\lambda) e^{(-\lambda_2 z)}] J_0(\lambda r) d\lambda\right]$$

for $-(H+ h_1+h_2) < z < -(H+h_1)$ (2.61)

$$\mathbf{F}_5 = C\left[\int_0^\infty [\psi_7(\lambda) e^{(\lambda_3 z)}] J_0(\lambda r) d\lambda\right] \text{ for } z < -(H+ h_1+h_2) \tag{2.62}$$

where $C = \frac{i\mu\omega\mathbf{M}}{4\pi}$ and ψ_1 to ψ_7 are functions of λ.

Making use of the Sommerfeld integral the exponential functions representing the primary vector potentials can be written as

$$\frac{e^{-k_0 R}}{R} = \int_0^\infty \frac{\lambda}{\lambda_0} e^{-\lambda_0 z} J_0(\lambda r) d\lambda \text{ for } z \geq 0 \tag{2.63}$$

$$\frac{e^{-k_0 R}}{R} = \int_0^\infty \frac{\lambda}{\lambda_0} e^{\lambda_0 z} J_0(\lambda r) d\lambda \text{ for } -H \leq z \leq 0 \tag{2.64}$$

Equations (2.58) – (2.62) can now be written as

$$\mathbf{F}_1 = C\left[\int_0^\infty [e^{-\lambda_0 z} + \psi_1(\lambda)e^{(-\lambda_0 z)}]J_0(\lambda r)d\lambda\right] \text{ for } z > 0 \qquad (2.65)$$

$$\mathbf{F}_2 = C\left[\int_0^\infty [e^{\lambda_0 z} + \psi_2(\lambda)e^{(-\lambda_0 z)}]J_0(\lambda r)d\lambda\right] \text{ for } -H < z < 0 \qquad (2.66)$$

$$\mathbf{F}_3 = C\left[\int_0^\infty [\psi_3(\lambda)e^{(\lambda_1 z)} + \psi_4(\lambda)e^{(-\lambda_1 z)}]J_0(\lambda r)d\lambda\right]$$

$$\text{for } -(H+h_1) < z < -H \qquad (2.67)$$

$$\mathbf{F}_4 = C\left[\int_0^\infty [\psi_5(\lambda)e^{(\lambda_2 z)} + \psi_6(\lambda)e^{(-\lambda_2 z)}]J_0(\lambda r)d\lambda\right]$$

$$\text{for } -(H+ h_1+h_2) < z < -(H+h_1) \qquad (2.68)$$

$$\mathbf{F}_5 = C\left[\int_0^\infty [\psi_7(\lambda)e^{(\lambda_3 z)}]J_0(\lambda r)d\lambda\right] \text{ for } z < -(H+ h_1+h_2) \qquad (2.69)$$

For the special case where $z = H = 0$ equations (2.65) - (2.69) can be expanded analytically to obtain expressions for the magnetic field components in the different regions (Keller and Frischknecht, 1966). We are however interested in finding solutions for the magnetic vector potentials if the transmitter loop is situated a distance above the ground. This will enable us to do theoretical modeling of airborne electromagnetic data. The only way to accomplish this is through numerical analysis.

From equations (2.36) and (2.37) we have the following boundary conditions

$$\frac{\partial \mathbf{F}_1}{\partial r} = \frac{\partial \mathbf{F}_2}{\partial r} \text{ and } \frac{\partial^2 \mathbf{F}_1}{\partial r \partial z} = \frac{\partial^2 \mathbf{F}_2}{\partial r \partial z} \text{ for } z = 0$$

$$\frac{\partial \mathbf{F}_2}{\partial r} = \frac{\partial \mathbf{F}_3}{\partial r} \text{ and } \frac{\partial^2 \mathbf{F}_2}{\partial r \partial z} = \frac{\partial^2 \mathbf{F}_3}{\partial r \partial z} \text{ for } z = -H$$

$$\frac{\partial \mathbf{F}_3}{\partial r} = \frac{\partial \mathbf{F}_4}{\partial r} \text{ and } \frac{\partial^2 \mathbf{F}_3}{\partial r \partial z} = \frac{\partial^2 \mathbf{F}_4}{\partial r \partial z} \text{ for } z = -(H+h_1)$$

$$\frac{\partial \mathbf{F}_4}{\partial r} = \frac{\partial \mathbf{F}_5}{\partial r} \text{ and } \frac{\partial^2 \mathbf{F}_4}{\partial r \partial z} = \frac{\partial^2 \mathbf{F}_5}{\partial r \partial z} \text{ for } z = -(H+h_1+h_2) \qquad (2.70)$$

Integration with respect to *r* yields the following equations. The constants of integration are all zero since the expressions must have zero value when *r* goes to infinity.

$$\mathbf{F}_1 = \mathbf{F}_2 \text{ and } \frac{\partial \mathbf{F}_1}{\partial z} = \frac{\partial \mathbf{F}_2}{\partial z} \text{ for } z = 0$$

$$\mathbf{F}_2 = \mathbf{F}_3 \text{ and } \frac{\partial \mathbf{F}_3}{\partial z} = \frac{\partial \mathbf{F}_4}{\partial z} \text{ for } z = -H$$

$$\mathbf{F}_3 = \mathbf{F}_4 \text{ and } \frac{\partial \mathbf{F}_3}{\partial z} = \frac{\partial \mathbf{F}_4}{\partial z} \text{ for } z = -(H+h_1)$$

$$\mathbf{F}_4 = \mathbf{F}_5 \text{ and } \frac{\partial \mathbf{F}_4}{\partial z} = \frac{\partial \mathbf{F}_5}{\partial z} \text{ for } z = -(h+h_1+h_2) \qquad (2.71)$$

Hence we can solve the functions ψ_1 to ψ_7 through a set of linear equations

$$e^{-\lambda_0 z} + \psi_1(\lambda) e^{(-\lambda_0 z)} = e^{\lambda_0 z} + \psi_2(\lambda) e^{(-\lambda_0 z)}$$

for $z = 0$ (2.72)

$$e^{\lambda_0 z} + \psi_2(\lambda) e^{(-\lambda_0 z)} = \psi_3(\lambda) e^{(\lambda_1 z)} + \psi_4(\lambda) e^{(-\lambda_1 z)}$$

for $z = -H$ (2.73)

$$\lambda_0 e^{\lambda_0 z} - \lambda_0 \psi_2(\lambda) e^{(-\lambda_0 z)} = \lambda_1 \psi_3(\lambda) e^{(\lambda_1 z)} - \lambda_1 \psi_4(\lambda) e^{(-\lambda_1 z)}$$

for $z = -H$ (2.74)

$$\psi_3(\lambda) e^{(\lambda_1 z)} + \psi_4(\lambda) e^{(-\lambda_1 z)} = \psi_5(\lambda) e^{(\lambda_2 z)} + \psi_6(\lambda) e^{(-\lambda_2 z)}$$

for $z = -(H+h_1)$ (2.75)

$$\lambda_1 \psi_3(\lambda) e^{(\lambda_1 z)} - \lambda_1 \psi_4(\lambda) e^{(-\lambda_1 z)} = \lambda_2 \psi_5(\lambda) e^{(\lambda_2 z)} - \lambda_2 \psi_6(\lambda) e^{(-\lambda_2 z)}$$

for $z = -(H+h_1)$ (2.76)

$$\psi_5(\lambda) e^{(\lambda_2 z)} + \psi_6(\lambda) e^{(-\lambda_2 z)} = \psi_7(\lambda) e^{(\lambda_3 z)}$$

for $z = -(H+h_1+h_2)$ (2.77)

$$\lambda_2 \psi_5(\lambda) e^{(\lambda_2 z)} - \lambda_2 \psi_6(\lambda) e^{(-\lambda_2 z)} = \lambda_3 \psi_7(\lambda) e^{(\lambda_3 z)}$$

for $z = -(H+h_1+h_2)$ (2.78)

For the case of a homogeneous halfspace we are left with 3 equations and 3 unknowns.

$$1 + \psi_1(\lambda) = 1 + \psi_2(\lambda) \quad (2.79)$$

$$e^{-(H)\lambda_0} + \psi_2(\lambda) e^{(H)(\lambda_0)} = \psi_3(\lambda) e^{-(H)(\lambda_1)} \quad (2.80)$$

$$\lambda_0 e^{-(H)\lambda_0} - \lambda_0 \psi_2(\lambda) e^{(H)(\lambda_0)} = \lambda_1 \psi_3(\lambda) e^{-(H)(\lambda_1)} \quad (2.81)$$

For the case of a two layered earth we have 5 equations and 5 unknowns

$$1 + \psi_1(\lambda) = 1 + \psi_2(\lambda) \quad (2.82)$$

$$e^{-(H)(\lambda_0)} + \psi_2(\lambda) e^{(H)(\lambda_0)} = \psi_3(\lambda) e^{-(H)(\lambda_1)} + \psi_4(\lambda) e^{(H)(\lambda_1)} \quad (2.83)$$

$$\lambda_0 e^{-(H)(\lambda_0)} - \lambda_0 \psi_2(\lambda) e^{(H)(\lambda_0)} = \lambda_1 \psi_3(\lambda) e^{-(H)(\lambda_1)} - \lambda_1 \psi_4(\lambda) e^{(H)(\lambda_1)} \quad (2.84)$$

$$\psi_3(\lambda) e^{-(H+h_1)(\lambda_1)} + \psi_4(\lambda) e^{(H+h_1)(\lambda_1)} = \psi_5(\lambda) e^{-(H+h_1)(\lambda_2)} \quad (2.85)$$

$$\lambda_1 \psi_3(\lambda) e^{-(H+h_1)(\lambda_1)} - \lambda_1 \psi_4(\lambda) e^{(H+h_1)(\lambda_1)} = \lambda_2 \psi_5(\lambda) e^{-(H+h_1)(\lambda_2)} \quad (2.86)$$

And finally, for a three layered earth model we have 7 equations with 7 unknowns

$$1+\psi_1(\lambda)=1+\psi_2(\lambda) \tag{2.87}$$

$$e^{-(H)\lambda_0}+\psi_2(\lambda)e^{(H)(\lambda_0)}=\psi_3(\lambda)e^{-(H)(\lambda_1)}+\psi_4(\lambda)e^{(H)(\lambda_1)} \tag{2.88}$$

$$\lambda_0 e^{-(H)\lambda_0}-\lambda_0\psi_2(\lambda)e^{(H)(\lambda_0)}=\lambda_1\psi_3(\lambda)e^{-(H)(\lambda_1)}-\lambda_1\psi_4(\lambda)e^{(H)(\lambda_1)} \tag{2.89}$$

$$\psi_3(\lambda)e^{-(H+h_1)(\lambda_1)}+\psi_4(\lambda)e^{(H+h_1)(\lambda_1)}=\psi_5(\lambda)e^{-(H+h_1)(\lambda_2)}+\psi_6(\lambda)e^{(H+h_1)(\lambda_2)} \tag{2.90}$$

$$\lambda_1\psi_3(\lambda)e^{-(H+h_1)(\lambda_1)}-\lambda_1\psi_4(\lambda)e^{(H+h_1)(\lambda_1)}=\lambda_2\psi_5(\lambda)e^{-(H+h_1)(\lambda_2)}-\lambda_2\psi_6(\lambda)e^{(H+h_1)(\lambda_2)} \tag{2.91}$$

$$\psi_5(\lambda)e^{-(H+h_1+h_2)(\lambda_2)}+\psi_6(\lambda)e^{(H+h_1+h_2)(\lambda_2)}=\psi_7(\lambda)e^{-(H+h_1+h_2)(\lambda_3)} \tag{2.92}$$

$$\lambda_2\psi_5(\lambda)e^{-(H+h_1+h_2)(\lambda_2)}-\lambda_2\psi_6(\lambda)e^{(H+h_1+h_2)(\lambda_2)}=\lambda_3\psi_7(\lambda)e^{-(H+h_1+h_2)(\lambda_3)} \tag{2.93}$$

The following square matrixes therefore have to be solved for the coefficients ψ_i to enable us to compute the magnetic field components.

For a halfspace:

$$\begin{bmatrix} 1 & -1 & 0 \\ 0 & e^{(H)(\lambda_0)} & -e^{-(H)(\lambda_1)} \\ 0 & -\lambda_0 e^{(H)(\lambda_0)} & -\lambda_1 e^{-(H)(\lambda_1)} \end{bmatrix} \begin{bmatrix} \psi_1(\lambda) \\ \psi_2(\lambda) \\ \psi_3(\lambda) \end{bmatrix} = \begin{bmatrix} 0 \\ -e^{-(H)(\lambda_0)} \\ -\lambda_0 e^{-(H)(\lambda_0)} \end{bmatrix} \tag{2.94}$$

For a two layered earth:

$$\begin{bmatrix} 1 & -1 & 0 & 0 & 0 \\ 0 & e^{(H)(\lambda_0)} & -e^{-(H)(\lambda_1)} & -e^{(H)(\lambda_1)} & 0 \\ 0 & -\lambda_0 e^{(H)(\lambda_0)} & -\lambda_1 e^{-(H)(\lambda_1)} & \lambda_1 e^{(H)(\lambda_1)} & 0 \\ 0 & 0 & e^{-(H+h_1)(\lambda_1)} & e^{(H+h_1)(\lambda_1)} & -e^{-(H+h_1)(\lambda_2)} \\ 0 & 0 & \lambda_1 e^{-(H+h_1)(\lambda_1)} & -\lambda_1 e^{(H+h_1)(\lambda_1)} & -\lambda_2 e^{-(H+h_1)(\lambda_2)} \end{bmatrix} \begin{bmatrix} \psi_1(\lambda) \\ \psi_2(\lambda) \\ \psi_3(\lambda) \\ \psi_4(\lambda) \\ \psi_5(\lambda) \end{bmatrix} = \begin{bmatrix} 0 \\ -e^{-(H)(\lambda_0)} \\ -\lambda_0 e^{-(H)(\lambda_0)} \\ 0 \\ 0 \end{bmatrix} \tag{2.95}$$

For a three layered earth:

$$\begin{bmatrix} 1 & -1 & 0 & 0 & 0 & 0 & 0 \\ 0 & e^{(H)(\lambda_0)} & -e^{-(H)(\lambda_1)} & -e^{(H)(\lambda_1)} & 0 & 0 & 0 \\ 0 & -\lambda_0 e^{(H)(\lambda_0)} & -\lambda_1 e^{-(H)(\lambda_1)} & \lambda_1 e^{(H)(\lambda_1)} & 0 & 0 & 0 \\ 0 & 0 & e^{-(H+h_1)(\lambda_1)} & e^{(H+h_1)(\lambda_1)} & -e^{-(H+h_1)(\lambda_2)} & -e^{(H+h_1)(\lambda_2)} & 0 \\ 0 & 0 & \lambda_1 e^{-(H+h_1)(\lambda_1)} & -\lambda_1 e^{(H+h_1)(\lambda_1)} & -\lambda_2 e^{-(H+h_1)(\lambda_2)} & \lambda_2 e^{(H+h_1)(\lambda_2)} & 0 \\ 0 & 0 & 0 & 0 & e^{-(H+h_1+h_2)(\lambda_2)} & e^{(H+h_1+h_2)(\lambda_2)} & -e^{-(H+h_1+h_2)(\lambda_3)} \\ 0 & 0 & 0 & 0 & \lambda_2 e^{-(H+h_1+h_2)(\lambda_2)} & -\lambda_2 e^{(H+h_1+h_2)(\lambda_2)} & -\lambda_3 e^{-(H+h_1+h_2)(\lambda_3)} \end{bmatrix} \begin{bmatrix} \psi_1(\lambda) \\ \psi_2(\lambda) \\ \psi_3(\lambda) \\ \psi_4(\lambda) \\ \psi_5(\lambda) \\ \psi_6(\lambda) \\ \psi_7(\lambda) \end{bmatrix} = \begin{bmatrix} 0 \\ -e^{-(H)\lambda_0} \\ -\lambda_0 e^{-(H)\lambda_0} \\ 0 \\ 0 \\ 0 \\ 0 \end{bmatrix} \tag{2.96}$$

From equations (2.34), (2.35) and (2.55) we can write expressions for the vertical and radial components of the magnetic field

$$i\mu\omega\mathbf{H}_z = k^2\mathbf{F} + \frac{\partial^2\mathbf{F}}{\partial z^2} \tag{2.97}$$

and

$$i\mu\omega\mathbf{H}_r = \frac{\partial^2\mathbf{F}}{\partial r \partial z} \tag{2.98}$$

We then have

$$\mathbf{H}_z = \frac{C}{i\mu\omega}\left[\int_0^\infty \left(\lambda_0{}^2 e^{\lambda_0 z} + \lambda_0{}^2 \psi_1(\lambda) e^{-\lambda_0 z}\right) J_0(\lambda r) d\lambda\right]$$

for $-H < z < 0$ (2.99)

with

$$J_0(\lambda r) = \frac{1}{\pi}\int_0^{\pi} cos(\lambda r \sin\theta)d\theta$$

$$\frac{\partial J_0(\lambda r)}{\partial r} = \frac{1}{\pi}\int_0^{\pi} -sin(\lambda r \sin\theta)(\lambda \sin\theta)d\theta$$ (Abramowitz and Stegun, 1964)

therefore

$$\mathbf{H}_r = \frac{C}{i\mu\omega}\left[\int_0^{\infty}\left[\left(\lambda_0 e^{\lambda_0 z} - \lambda_0\psi_2(\lambda)e^{-\lambda_0 z}\right)\cdot\left(\frac{1}{\pi}\int_0^{\pi}(-sin(\lambda r \sin\theta)(\lambda \sin\theta))d\theta\right)\right]d\lambda\right]$$

for $-H < z < 0$ (2.100)

Although the above expression describes the vertical and radial component of the electromagnetic field response for a layered earth perfectly, we still face a problem if we want to use these expressions in the formulation of an inversion routine. The construction of the Jacobian matrix (see Section 4) necessitates the calculation of the partial derivatives of equations (2.99) and (2.100) with respect to all the model parameters that needs to be resolved through the inversion process. Numerical calculation of the partial derivatives is not ideal since numerical inaccuracies in the determination of the derivatives will render the inversion process unstable (Huang and Fraser, 2003).

In Section 3 we will therefore adopt the approach by Ward and Hohmann (1988) who defines the electromagnetic field components in terms of a

recursive reflection coefficient r_{TE}. This will enable us to determine the partial derivatives analytically.

3. FORWARD MATHEMATICAL DESCRIPTION FOR DETERMINING THE ELECTROMAGNETIC FIELD RESPONSE OF A CONDUCTIVE AND MAGNETICALLY SUSCEPTIBLE LAYERED EARTH.

Ward and Hohmann (1988) defines the electromagnetic field components in terms of a recursive reflection coefficient r_{TE} which enables one to compute the partial derivatives of the field response with respect to the different model parameters. **Please note the slight change in the reference coordinate system from Section 2.** The surface of the conductive halfspace is situated at $z = 0$ and the z axis point negative up with its origin at the surface. There is also a change in notation from r to ρ (Figure 3.1). **This ρ must not be mistaken for resistivity since ρ is often used in literature for resistivity**.

A general solution for the EM field components above a horizontally layered earth for a vertical magnetic dipole in cylindrical coordinates is now given by Ward and Hohmann (1988) p. 209:

$$H_\rho = \frac{\mathbf{M}}{4\pi}\int_0^\infty (e^{-Y_0(z+L)} - r_{TE}e^{Y_0(z-L)})\lambda^2 J_1(\lambda\rho)d\lambda \qquad (3.1)$$

and

$$H_z = \frac{\mathbf{M}}{4\pi}\int_0^\infty (e^{-Y_0(z+L)} + r_{TE}e^{Y_0(z-L)})\frac{\lambda^3}{Y_0} J_0(\lambda\rho)d\lambda \qquad (3.2)$$

With,

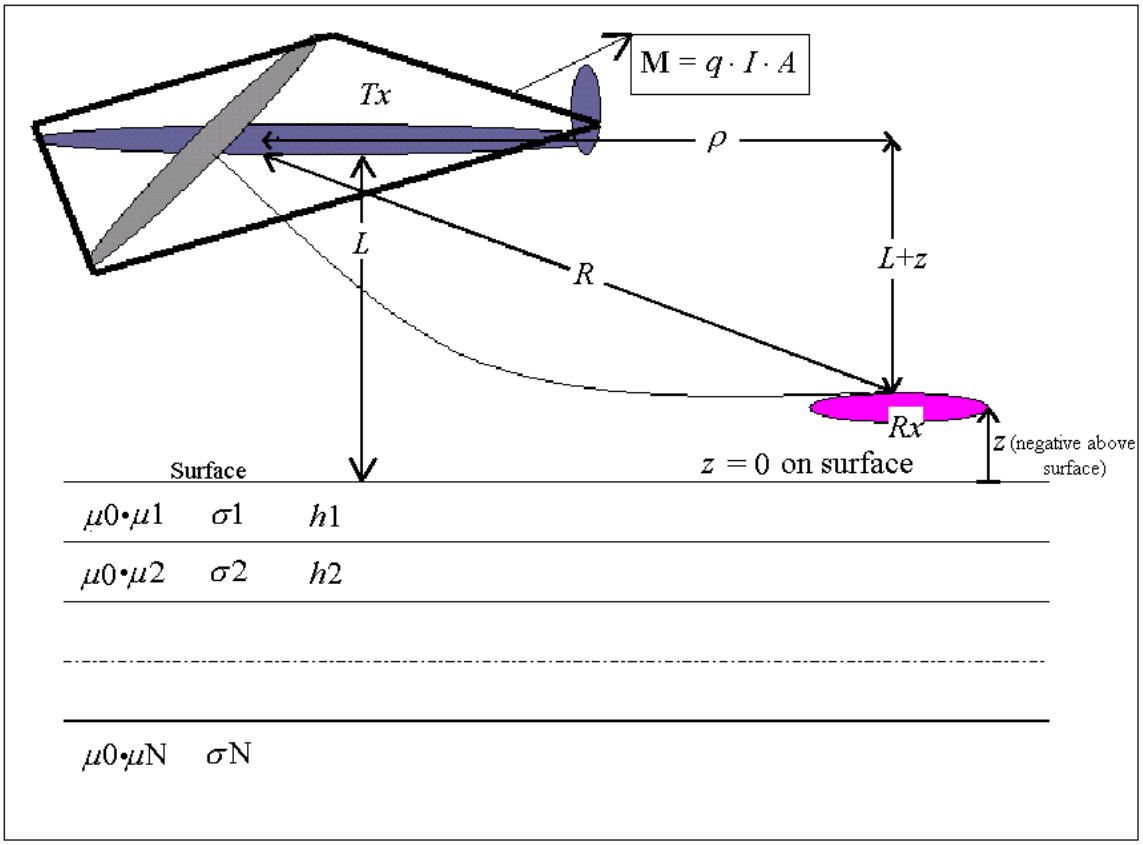

Figure 3.1. Reference system for the airborne electromagnetic platform.

H_ρ the radial component of the magnetic field, H_z the vertical component of the magnetic field, **M** the dipole moment of the transmitter loop with **M** = qIAâ, z the observation position (receiver position) with the origin of the coordinate system being on the surface indicating positive down, L the height of the source (transmitter), J_1 the Bessel function of the first kind of order one, J_0 the Bessel function of the first kind of order zero, λ the integration variable and ρ is the horizontal dipole separation.

r_{TE} is the reflection coefficient and is given by Ward and Hohmann (1988) p. 205:

$$r_{TE} = \frac{Y_0 - Y_1^{'}}{Y_0 + Y_1^{'}} \tag{3.3}$$

$$Y_n^{'} = Y_n \frac{Y_{n+1}^{'} + Y_n \tanh((\lambda^2 + k_n^2)^{1/2} h_n)}{Y_n + Y_{n+1}^{'} \tanh((\lambda^2 + k_n^2)^{1/2} h_n)} \tag{3.4}$$

with n =1,2,…..,N-1 for a N layered earth where,

$$Y_n = (\lambda^2 + k_n^2)^{1/2}$$

and

$$Y_0 = (\lambda^2 + k_0^2)^{1/2} \tag{3.5}$$

and the wave number for the n^{th} layer is given by

$$k_n^2 = (i\omega\mu_0\mu_n\sigma_n - \omega^2\mu_0\mu_n\varepsilon_0) \tag{3.6}$$

where h_n is the **thickness**, μ_n is the magnetic permeability of the n^{th} layer divided by μ_0 and σ_n is the conductivity of the n^{th} layer. Furthermore, ω is

the angular frequency of the source current and ε_0 is the dielectric permittivity of free space.

For a quasi-static approximation the wave number becomes

$$k_n^2 = (i\omega\mu_0\mu_n\sigma_n) \qquad (3.7)$$

At the bottom of the layered earth we have a half-space and hence we can write $Y_N^{'} = Y_N$

We can now generate an expression for $Y_1^{'}$ by making use of the recursive relation in equation (3.4).

As for the solution in Section 2, an analytic solution can be found for the special case where the transmitter and receiver are situated on the surface of the earth. Modern day computing power enables us however to solve the equations numerically for the transmitter and receiver in the air. Once the model parameters are specified the integral in equations (3.1) and (3.2) can be solved. If however the transmitter and receiver are situated on the ground equations (3.1) and (3.2) have a slowly divergent and oscillating nature with respect to the integration variable λ. A method proposed by Anderson (1979) is widely used for the integration of Hankel Transforms and yields a rapidly converging result if the function is oscillating and slowly convergent. The generality of these equations also implies that the proposed algorithm can be applied equally well to either an airborne or a ground based EM system.

In order to gain more insight into relative changes that can be expected in the observed data for a change in the layered earth model a few standard

curves are drawn. It is very useful at this stage to define a model response parameter $W = \frac{\rho}{\left(\frac{2}{\sigma_1 \mu_0 \omega}\right)^{1/2}}$ and a mutual coupling ratio $\frac{\mathbf{Z}_z}{\mathbf{Z}_0} = \frac{(\mathbf{H}_{s+p})_z}{(\mathbf{H}_p)_z}$ (Frischknecht, 1967). The dimensionless property of W enables us to compile a set of standard curves to use for our system under consideration.

For the specific case of a co-planar system situated above a homogeneous earth the curves in Figure 3.2a can be generated if the magnetic susceptibility of the halfspace is equal to that of free-space. X is defined as $X = \frac{|z| + L}{\left(\frac{2}{\sigma_1 \mu_0 \omega}\right)^{1/2}}$ and hence $\frac{X}{W} = \frac{2L}{\rho}$ for a co-planar system. For a fixed dipole separation the response is therefore effectively calculated for different heights of the co-planar dipole above the surface of a homogeneous halfspace. These curves are identical to those generated by Frischknecht (1967) (Figure 3.2b). Frischknecht however used slightly different symbols where X = A, W = B, x = k and D = D.

Figure 3.3 depicts the FDEM response over a two-layered earth. $D = \frac{2h_1}{\left(\frac{2}{\sigma_1 \mu_0 \omega}\right)^{1/2}}$ with h_1 the thickness of the first layer and $\frac{D}{W} = \frac{2h_1}{\rho}$. We

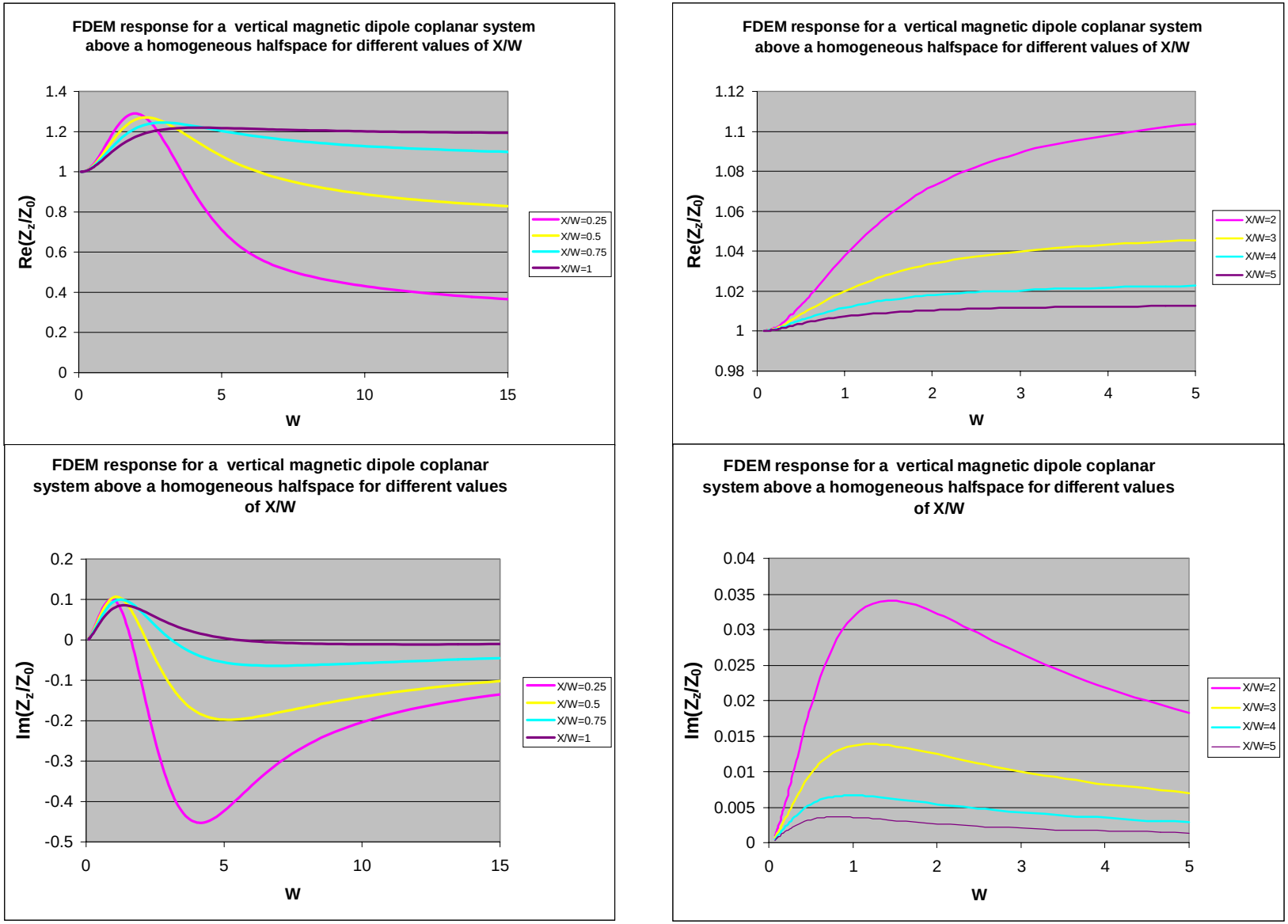

Figure 3.2a.FDEM response for a vertical magnetic dipole coplanar system above a homogeneous halfspace for different values of X/W.

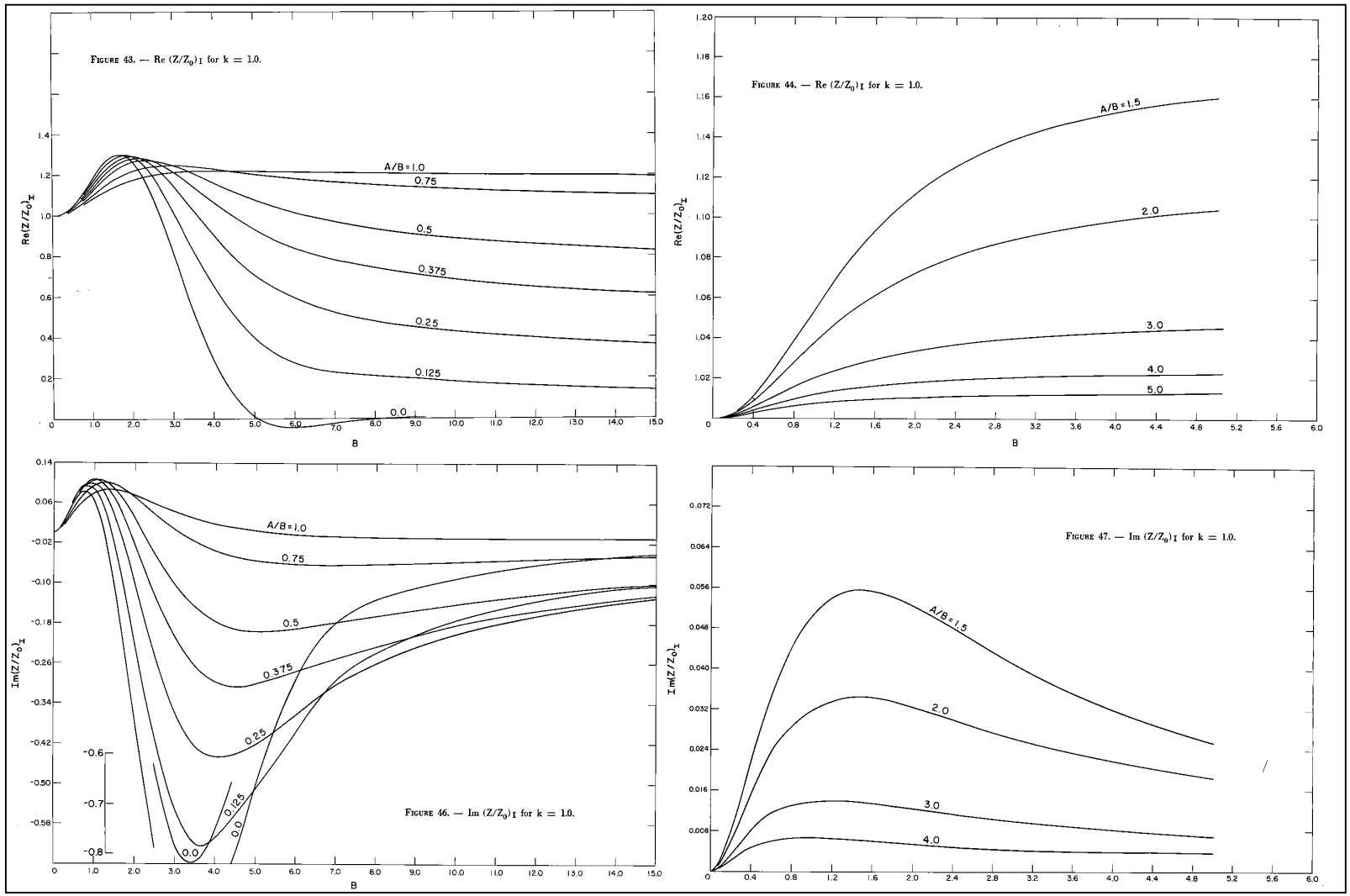

Figure 3.2b. Curves generated by Frischknecht (1967) shown to validate the curves in Figure 3.2a. Please note that A = X and B = W (from Frischknecht 1967).

also define x as the ratio $\frac{\sigma_2}{\sigma_1}$. If X/W and D/W are kept constant we can change x and observe the change in the FDEM response at the receiver due to a change in subsurface conductivity distribution.

Figure 3.4 and Figure 3.5 uses the system geometry as shown in Figure 3.1. The transmitter is at a fixed height of 100m. The receiver is towed in a bird 30m behind and 50m below the aircraft. In Figure 3.4 X/W and x are kept constant. If ρ is also constant a change in D/W implies a change in the thickness of the first layer. Figure 3.4 then indicates the variation in the observed FDEM response for a given change in the thickness of the first layer of a two-layered model.

In Figure 3.5 the thickness of the first layer is fixed at 20m and that of the second layer at 10m. Five models, each with a different conductivity distribution, are being considered. From the curves it is obvious that a conductive second layer situated within a resistive host rock can be much better resolved than a resistive second layer situated in a conductive host rock.

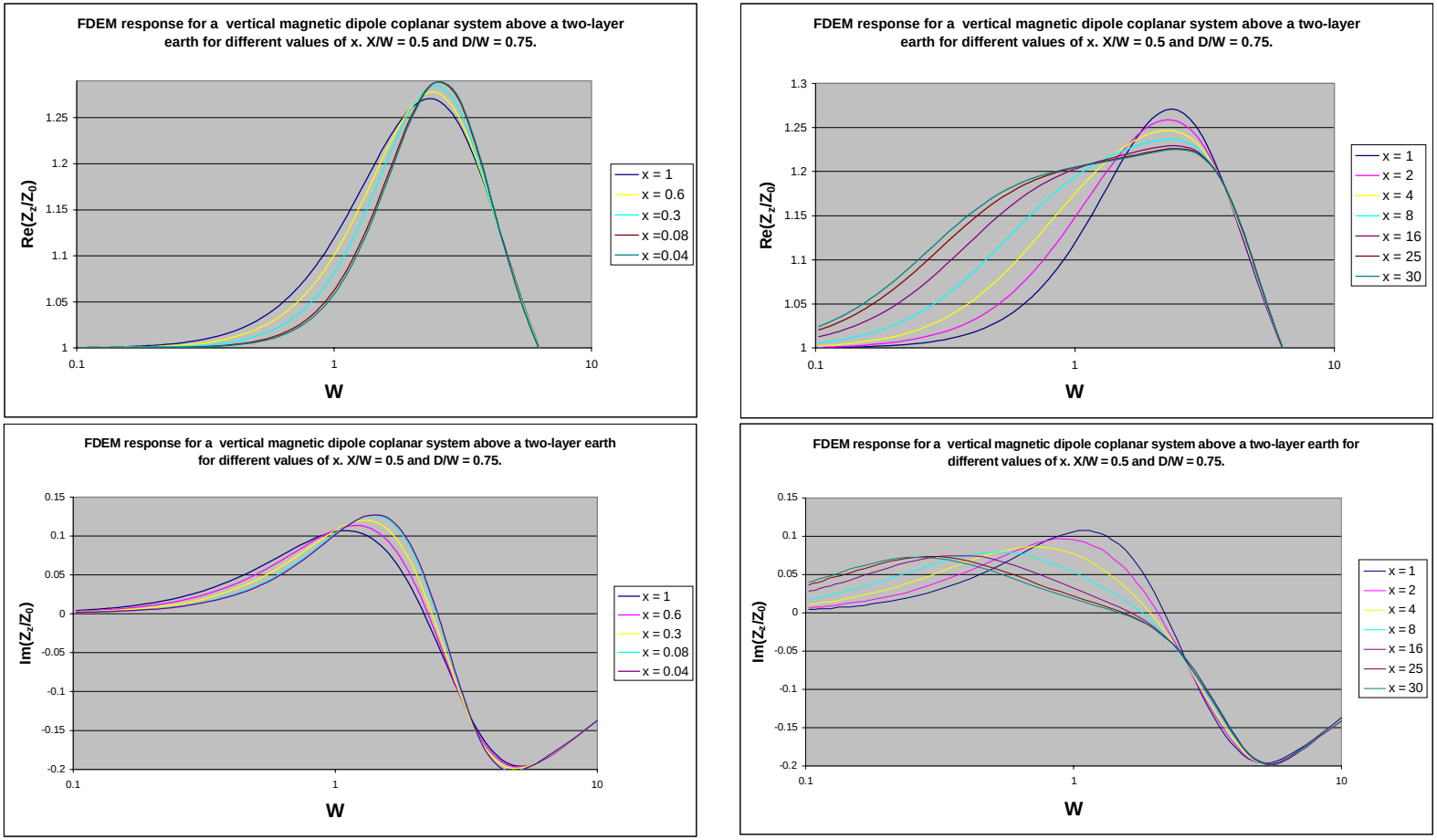

Figure 3.3. FDEM response for a vertical magnetic dipole coplanar system above a two-layer earth for different values of x. X/W = 0.5 and D/W = 0.75.

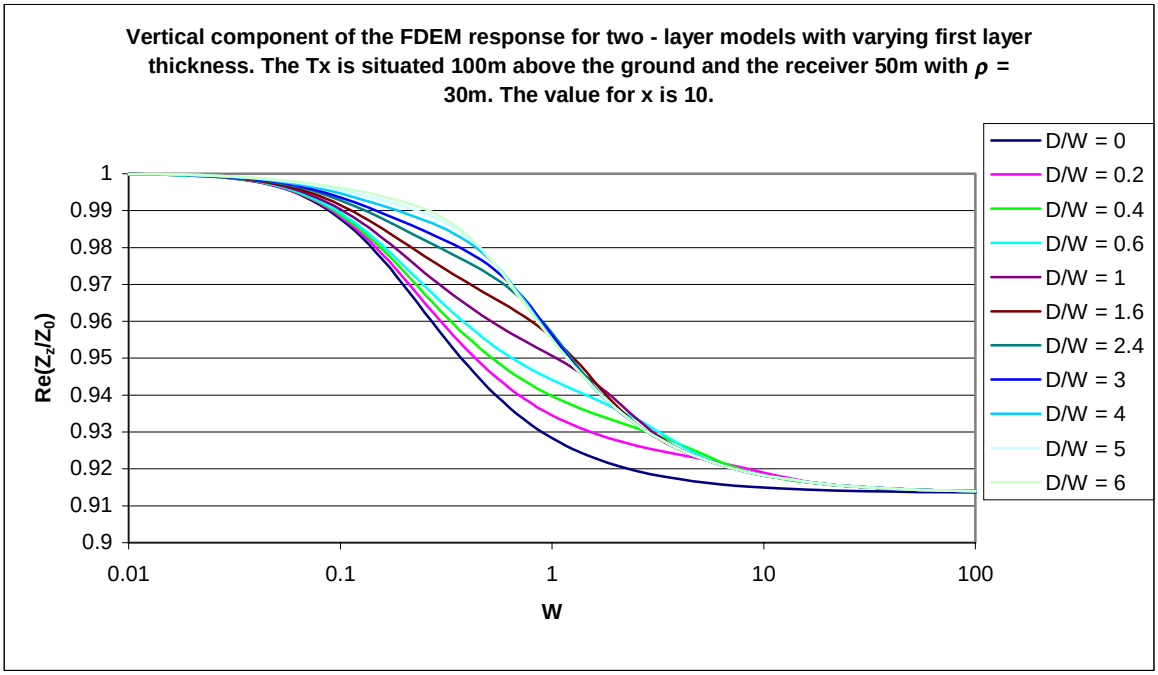

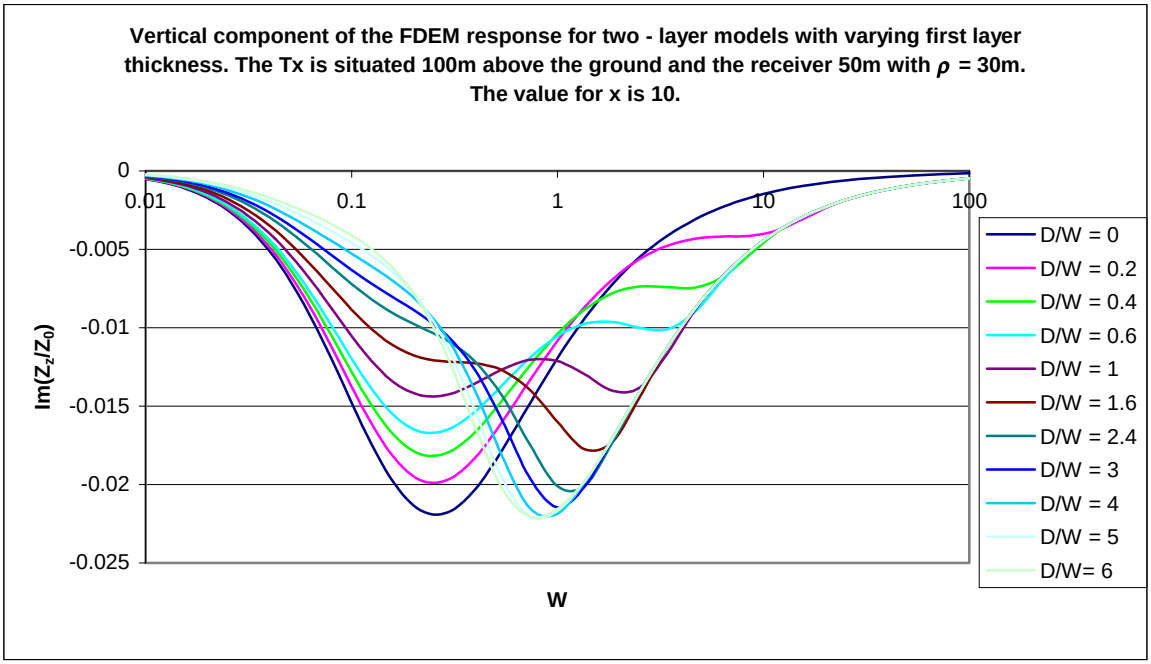

Figure 3.4. Vertical component of the FDEM response for two-layer models with varying first layer thickness.

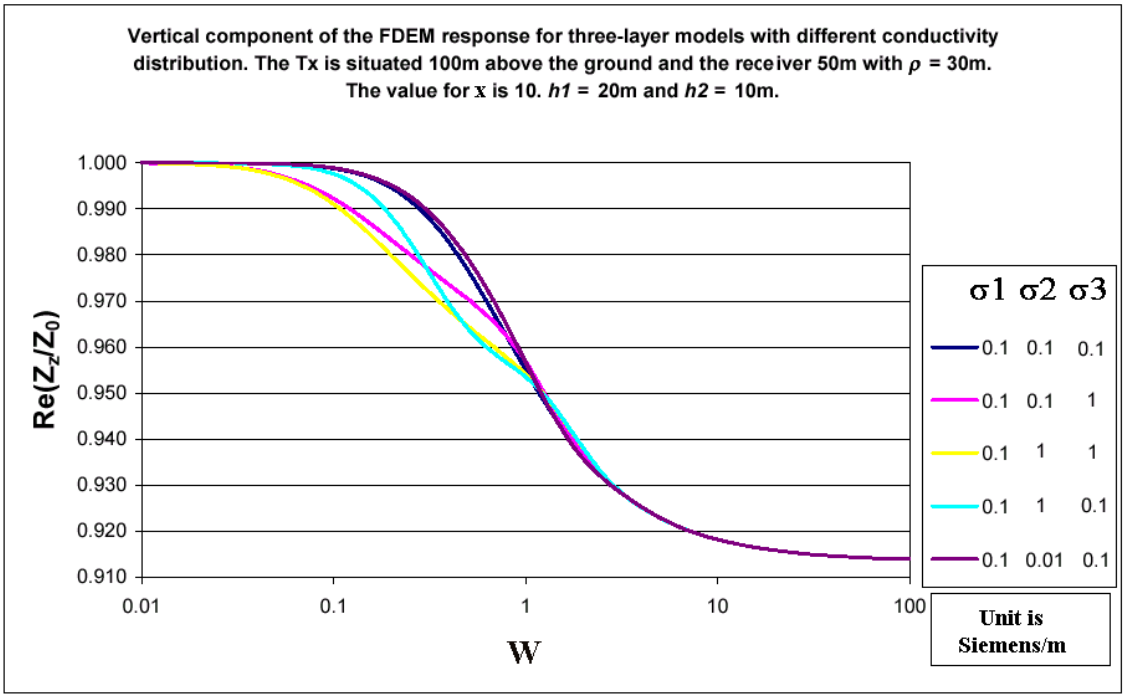

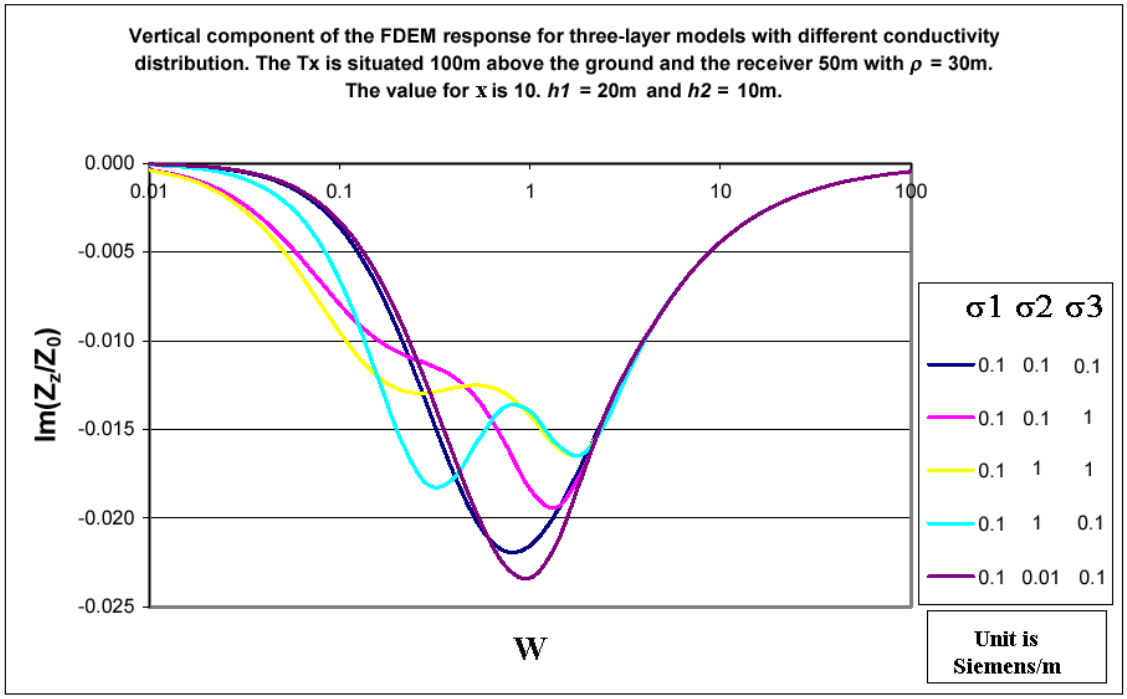

Figure 3.5. Vertical component of the FDEM response for three-layer models with varying layer conductivities.

4. INVERSION METHODOLOGY

4.1. DAMPED LEAST SQUARES INVERSION

A data vector **d** and a model parameter vector **p** can be defined where **d** = $[d_1,d_2,\ldots,d_N]^T$ for N observations and **p** = $[p_1,p_2,\ldots,p_M]^T$ for M model parameters. The measured data can now be related to the model parameters by:

$$d_i = F_i(\mathbf{p}),\ i = 1,2,\ldots,N. \tag{4.1}$$

Since $F_i(\mathbf{p})$ is a highly non-linear function we expand $F_i(\mathbf{p})$ in a Taylor series around an initial model parameter vector $\mathbf{p}^0$ for the first iteration and neglect higher order terms (Lines and Treitel, 1984). Equation (4.1) then becomes

$$(d_i - d_i^0) = \sum_{j=1}^{M} \frac{\partial F_i(\mathbf{p}^0)}{\partial p_j}(p_j - p_j^0) \tag{4.2}$$

where the vector $\mathbf{d}^0$ is the system response due to the initial model parameter vector $\mathbf{p}^0$.

The error between the observed and calculated data is given as

$$\mathbf{e} = \mathbf{d} - F(\mathbf{p}) \tag{4.3}$$

and

$$\Delta\mathbf{d} = \mathbf{J}\Delta\mathbf{p} \tag{4.4}$$

J is an NxM matrix called the Jacobian partial derivative matrix and is given by

$$j_{ik} = \frac{\partial F_i}{\partial p_k},\ i = 1,2,\ldots N \text{ and } k = 1,2,\ldots,M. \tag{4.5}$$

If we minimize the cumulative least square error relative to the parameter change vector we obtain

$$\Delta \mathbf{p} = (\mathbf{J}^{\mathbf{T}}\mathbf{J})^{-1}\mathbf{J}^{\mathbf{T}}\Delta \mathbf{d} \qquad (4.6)$$

Next we apply singular value decomposition (SVD) to **J,** so we can write $\mathbf{J} = \mathbf{U}\Lambda\mathbf{V}^{\mathbf{T}}$ where **U** is an NxM data eigenvector matrix, **V** is an MxM parameter eigenvector matrix, and Λ is an MxM diagonal matrix with elements λ_k also known as singular values. A new expression for the parameter change vector can now be obtained

$$\Delta \mathbf{p} = \mathbf{V}\Lambda^{-1}\mathbf{U}^{\mathbf{T}}\Delta \mathbf{d} \qquad (4.7)$$

If $1/\lambda_k$ becomes too large, numerical instability becomes a problem. Marquardt (1963) employed a damping factor β to stabilize the inversion. With Marquardt's damping factor equation (4.7) reduces to

$$\Delta \mathbf{p} = \mathbf{V}\Lambda(\Lambda^{2} + \beta\mathbf{I})^{-1}\mathbf{U}^{\mathbf{T}}\Delta \mathbf{d} \qquad (4.8)$$

A large damping factor would apply more constraint to a solution and give poor resolution of the parameters. A small damping factor may create instability in the inversion. Another problem is that all the parameters are not equally resolvable hence the need arises for a spatially variable damping factor that assigns a damping factor to each parameter based on its resolvability and updates the factors after each iteration. A method that addresses this problem is called active constrained balancing (ACB) and is described by Yi et al. (2003).

An updated model parameter vector after *j* iterations is now given by $\mathbf{p}^{j} = \mathbf{p}^{j-1} + \Delta\mathbf{p}$. The error will be minimized in a least squares sense until an acceptable fit to the data vector is obtained.

All the parameters that we need to invert for are contained in the reflection coefficient. Determining the partial derivatives needed to construct the Jacobian matrix thus simply entail determining the partial derivatives of the reflection coefficient with respect to every model parameter. Following Huang and Fraser (2003) the partial derivatives are solved analytically using the chain rule.

$$\frac{\partial r_{TE}}{\partial p_j} = \frac{\partial r_{TE}}{\partial Y_1^{'}} \frac{\partial Y_1^{'}}{\partial p_j} = \frac{-2Y_0}{(Y_0 + Y_1^{'})^2} \cdot \frac{\partial Y_1^{'}}{\partial p_j} \tag{4.9}$$

and for the specific case of a three layered earth we have

$$\frac{\partial Y_1^{'}}{\partial p_j} = \frac{\partial Y_1^{'}}{\partial Y_2^{'}} \cdot \frac{\partial Y_2^{'}}{\partial Y_3^{'}} \cdot \frac{\partial Y_3^{'}}{\partial p_j}, \quad \frac{\partial Y_1^{'}}{\partial p_j} = \frac{\partial Y_1^{'}}{\partial Y_2^{'}} \cdot \frac{\partial Y_2^{'}}{\partial p_j} \text{ and } \frac{\partial Y_1^{'}}{\partial p_j} = \frac{\partial Y_1^{'}}{\partial p_j} \tag{4.10}$$

for parameters in the last, second and first layer respectively and from equation (3.4),

$$\frac{\partial Y_1^{'}}{\partial Y_2^{'}} = \frac{(Y_1)^2 (1 - \tanh^2((\lambda^2 + k_1^2)^{1/2} \cdot h_1))}{(Y_1 + Y_2^{'} \tanh((\lambda^2 + k_1^2)^{1/2} \cdot h_1))^2}$$

and

$$\frac{\partial Y_2^{'}}{\partial Y_3^{'}} = \frac{(Y_2)^2 (1 - \tanh^2((\lambda^2 + k_2^2)^{1/2} \cdot h_2))}{(Y_2 + Y_3^{'} \tanh((\lambda^2 + k_2^2)^{1/2} \cdot h_2))^2} \tag{4.11}$$

The partial derivatives of the AEM response with respect to model parameters can now be calculated but since AEM data and model parameters vary over several orders of magnitude, data and model parameters have to be re-scaled to $\log_e d_i$ and $\log_e p_k$ (Jupp and Vozoff, 1975). By applying a logarithmic re-scaling of model parameters one also introduces a natural positivity constraint on the solution which then circumvents any meaningless

negative results in either layer thickness or layer conductivities. The new model parameter vector is defined as $\mathbf{x} = [\ln(p_1), \ln(p_2), \ldots, \ln(p_M)]^T$ and the Jacobian is given by:

$$\mathbf{J}_{i,k} = \frac{\partial F_i}{\partial x_k} = \frac{\partial F_i}{\partial \ln p_k} = p_k \cdot \frac{\partial F_i}{\partial p_k} \text{ for } i = 1,2,\ldots N \text{ and } k = 1,2,\ldots,M. \quad (4.12)$$

Analysis of the partial derivatives can yield valuable information about the resolvability of parameters during inversion. Relative high amplitudes would indicate that a small change in the parameter would result in a large variation in measured data. Relative low amplitudes would indicate that the parameter is poorly resolved and an accurate parameter determination would become difficult. Analysis of partial derivatives is also of practical importance to the interpretation of airborne Time Domain EM data. TDEM data does not have the problem of an intrinsic lack of frequencies which is the case for a FDEM system where one is limited by the system design to a few frequencies. By analyzing the partial derivatives for the different parameters along the frequency spectrum one can get a good idea where variation in the observed data could be expected for a certain change in model parameters. Consequently, the algorithm can be fine tuned by selecting only those frequencies that will optimize the resolving power of the inversion process. An alternative to evaluating the partial derivatives would be to investigate $\mathbf{J} = \mathbf{U}\Lambda\mathbf{V}^{\mathbf{T}}$ further. Here, parameters associated with large singular values (λ_k) are best determined while parameters associated with small singular values are poorly resolved.

The starting model for an inversion can usually be generated with an imaging algorithm as described in Section 1. Using the initial parameters from the starting model the secondary frequency domain response associated with the initial model is calculated. After each inversion the misfit between the measured data and the model response is calculated. As soon as the misfit is acceptable the new physical model is used as starter model for the next sounding.

4.2. INVERSION OF NOISE-FREE SYNTHETIC DATA.

The synthetic model chosen for the implementation of the three-layer inversion algorithm is that of a typical palaeo-channel associated with alluvial diamond deposits (Figure 4.1). Using a three-layer forward algorithm based on equation (3.2) the electromagnetic response was determined for a coplanar system with a dipole separation of 10m and a ground clearance of 40m above the physical model.

The misfit is defined as $\frac{\sum_{i=1}^{N}(d_i - F_i(\mathbf{p}))^2}{N}$. In this section the z component of the secondary induced magnetic field response plus the z component of the primary magnetic field is normalized with the z component of the primary magnetic field. The misfit is then given in $(\text{parts})^2$.

The starting model for every station along the profile is kept the same in Figures 4.2b - 4.2f to showcase the robustness of the technique if no information is available on the subsurface geology. The process is stopped

after 5 iterations when the initial physical model is almost completely recovered.

Figure 4.3 is produced by implementing a more practical approach. The starting model for the first station, which in practice can be obtained through borehole information or a conductivity depth transform of the field data, is: h_1 = 4 m, σ_1 = 0.004 S/m, h_2 = 10 m, σ_2 = 0.06 S/m and σ_3 = 0.0025 S/m.

The inversion process for all stations stop as soon as the misfit falls below $1 \cdot 10^{-14}$ $(\text{parts})^2$. When this criteria is met at the first station the model obtained is transferred to the next station. This model is then used as the new starting model for the second station. Initially, at the first few stations, the number of iterations required to obtain an acceptable misfit is quite high but the number of iterations soon decrease. The amount of iterations needed to successfully map the conductivity structure of the central part of the data segment therefore decreases from (5-6) to (2-3). The number of iterations again increase close to the edge of the data segment since the frequencies selected in generating the synthetic data was kept constant throughout the data segment. These frequencies however are not optimal in resolving the given model parameters close to the edge of the data segment and in practice these optimal frequencies can be selected from the raw field data for every station before an inversion is attempted, if this is practical.

4.3. INVERSION OF NOISY SYNTHETIC DATA.

A percentage of noise was added to the chosen frequencies to simulate either noise or effects that could be attributed to three-dimensional structures. The

variation at each frequency along the profile is shown in Figure 4.4a. The cumulative effect over all five frequencies constitutes a noise level of 8-10%. The same methodology is followed as in Figure 4.3 where the starting model is taken from the previous station. Due to the noise levels in the data the minimum misfit requirement was not met and the maximum amount of iterations (5) were applied at all stations. The inversion results are shown in Figure 4.4b.

Appendix A contains the "Mathcad" code that was developed for the implementation of a two-layer damped least-squares inversion algorithm. The algorithm is constructed to invert single stations for a given starting model.

Synthetic data from a publication by Huang and Fraser (1996) p. 108 is used as input for the program. The model is a 2-layered earth where h_1 = 10m, σ_1 = 0.02 S/m and σ_2 = 0.001 S/m. The ppm amplitudes from Huang and Fraser (1996) must be multiplied by 2 before the inversion. This is because they normalized their secondary magnetic field with respect to the x-component of the primary field and the mathematics in this algorithm assumes normalization with respect to the z-component.

The response is calculated from the model at the three specified frequencies of 57600 Hz, 14400 Hz and 1800 Hz and is 1423 ppm, 894.6 ppm and 160.4 ppm consecutively. Using a starting model where $_{\eta 1}$ = 5μ, σ_1 = 0.05 S/m and σ_2 S/m = 0.005 the true model is almost completely recovered after just 6 iterations.

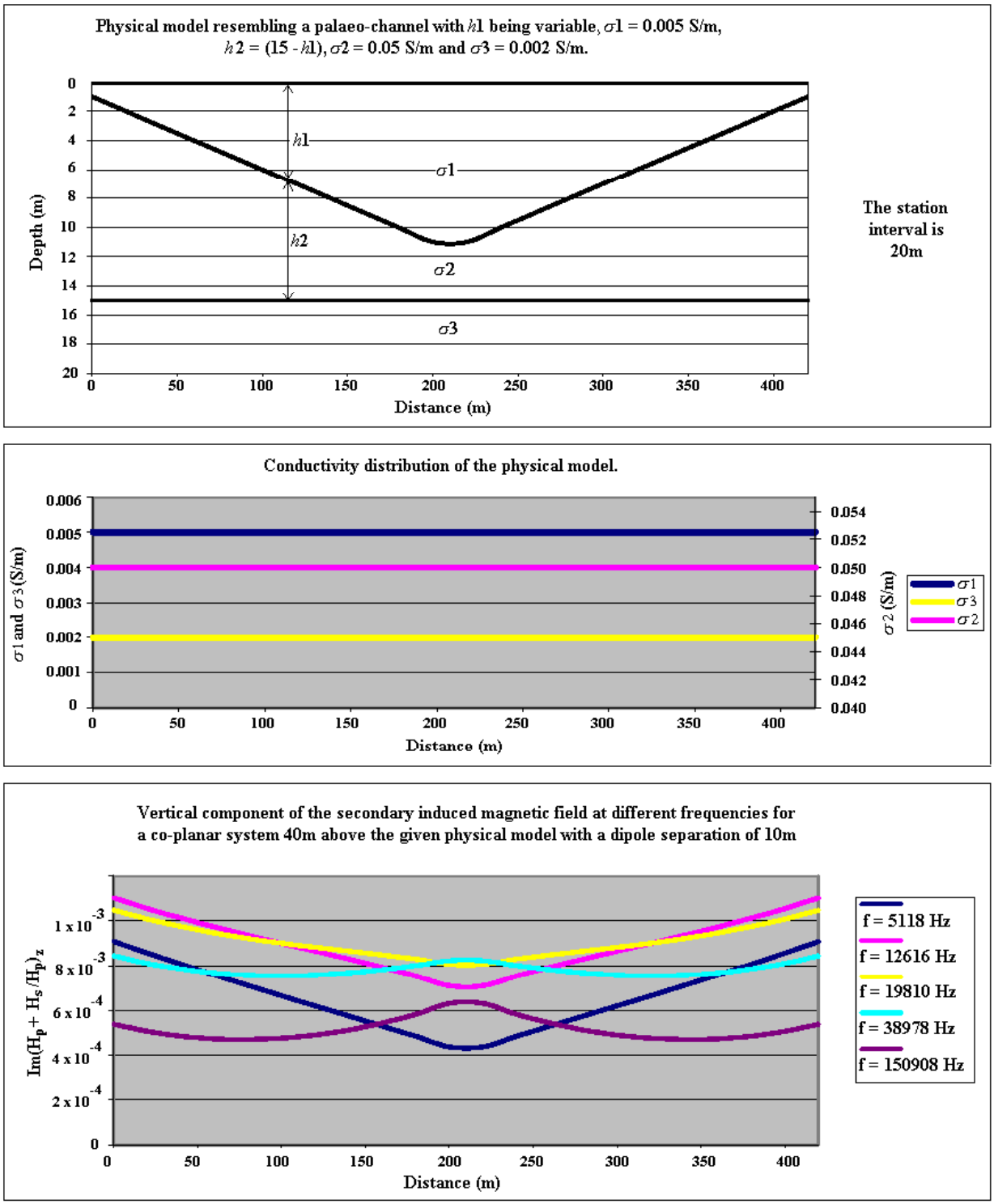

Figure 4.1. Physical model used to generate synthetic data for the 3-layer damped least-squares inversion of airborne electromagnetic data.

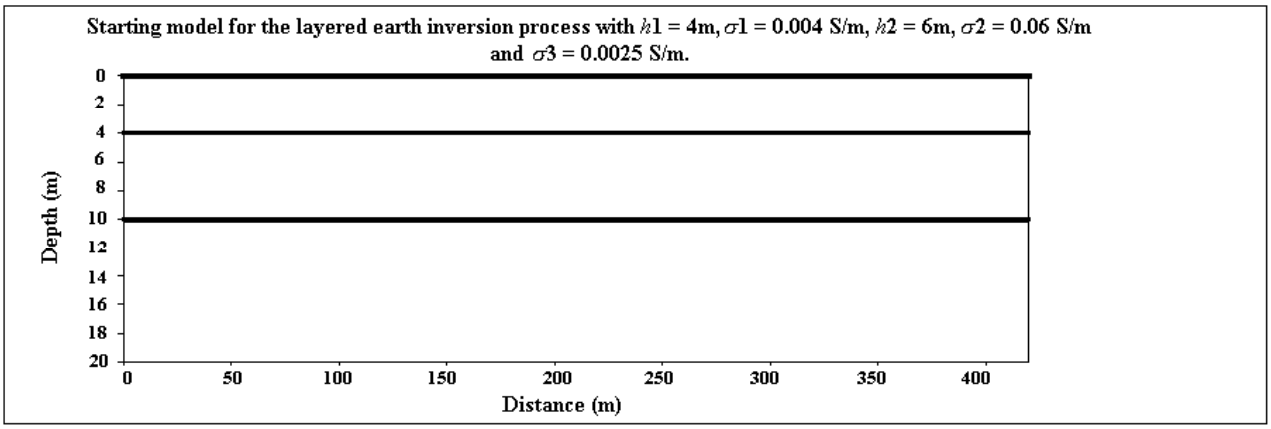

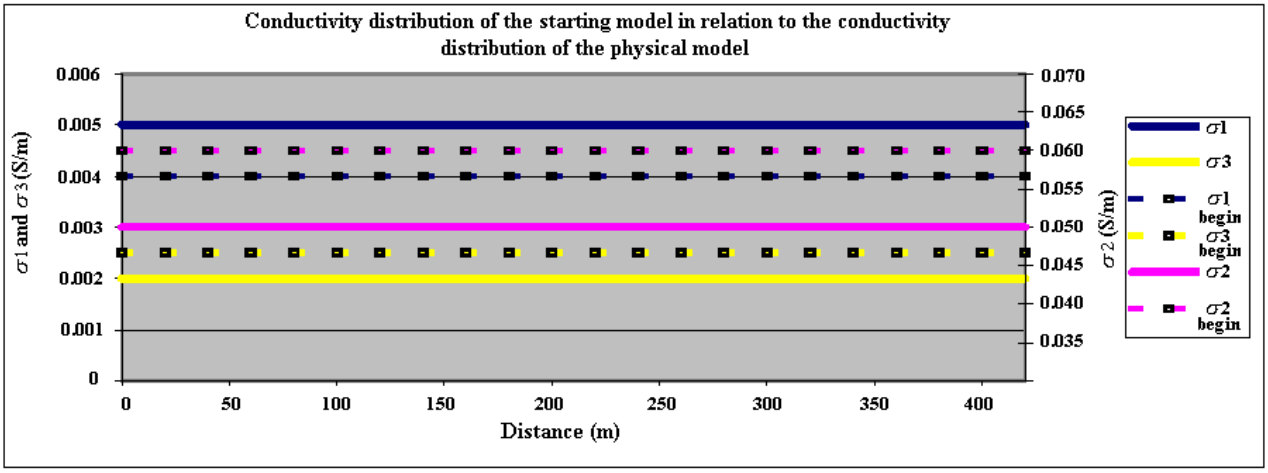

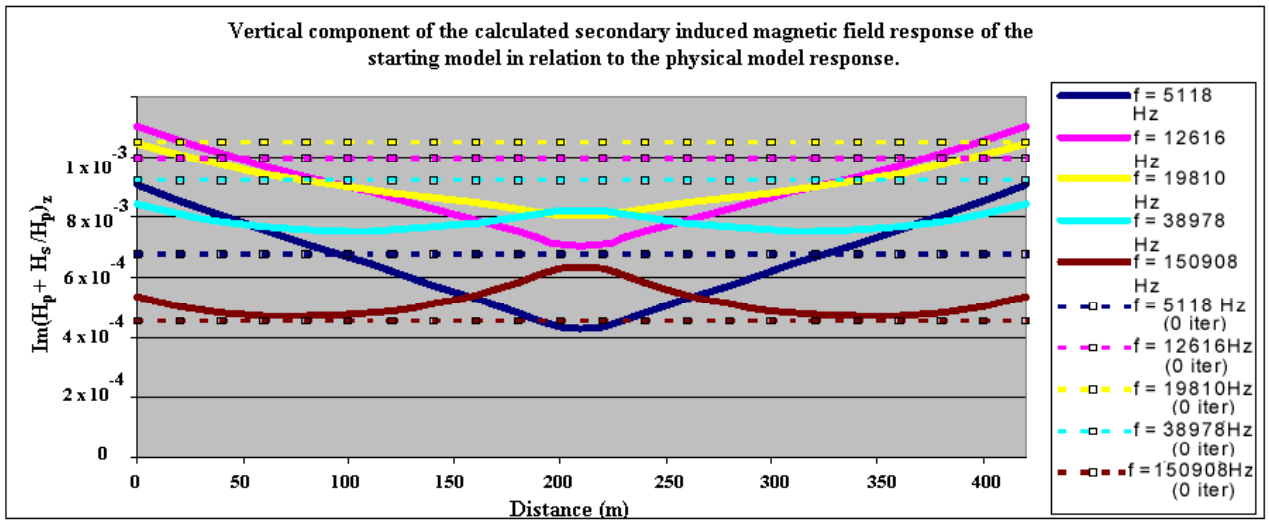

Figure 4.2a. Starting model for the layered earth inversion. The same starting model is used at each station.

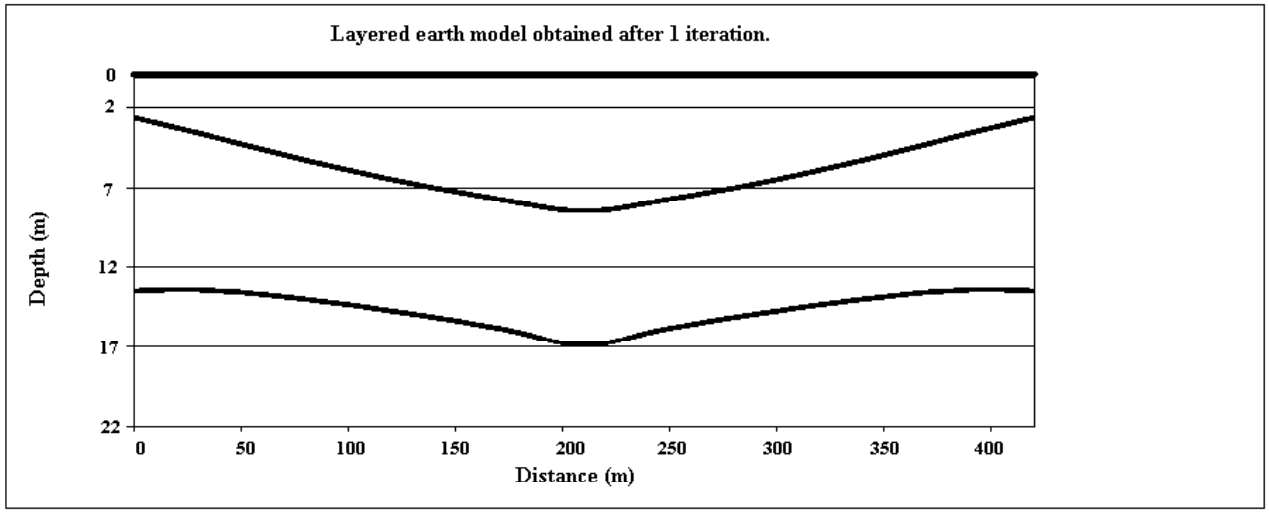

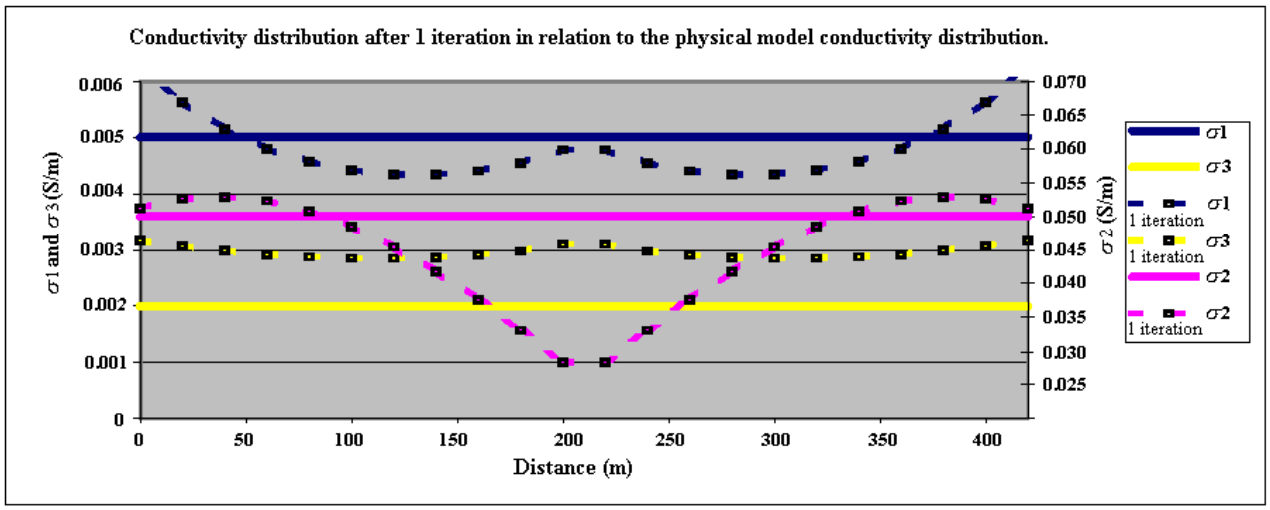

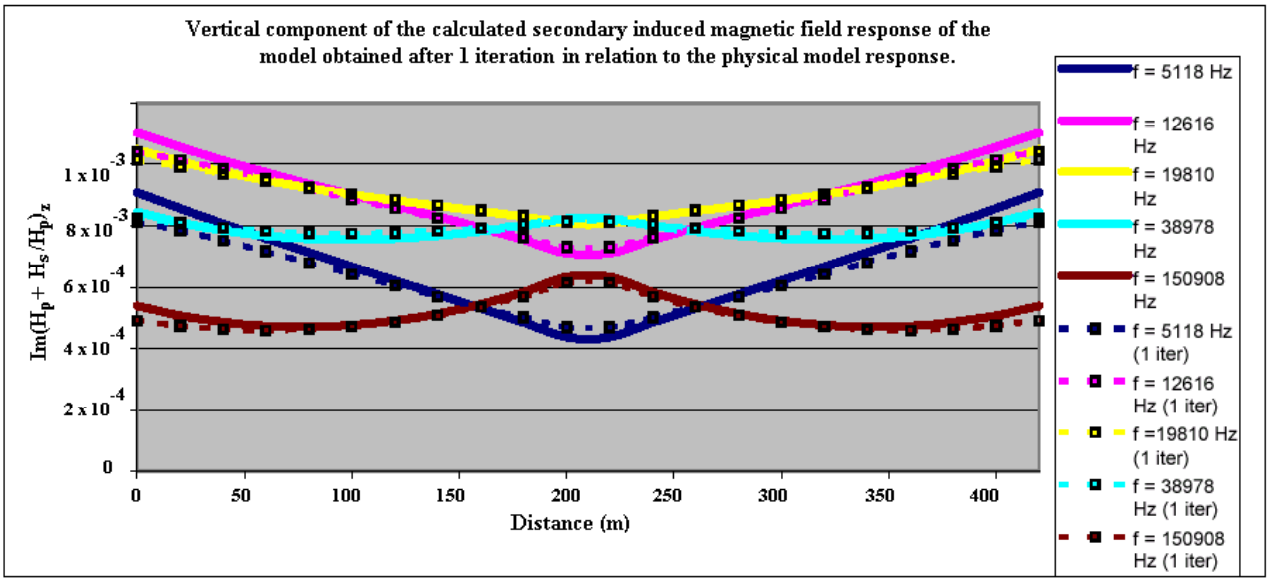

Figure 4.2b. Three-layer model obtained along the profile after 1 iteration.

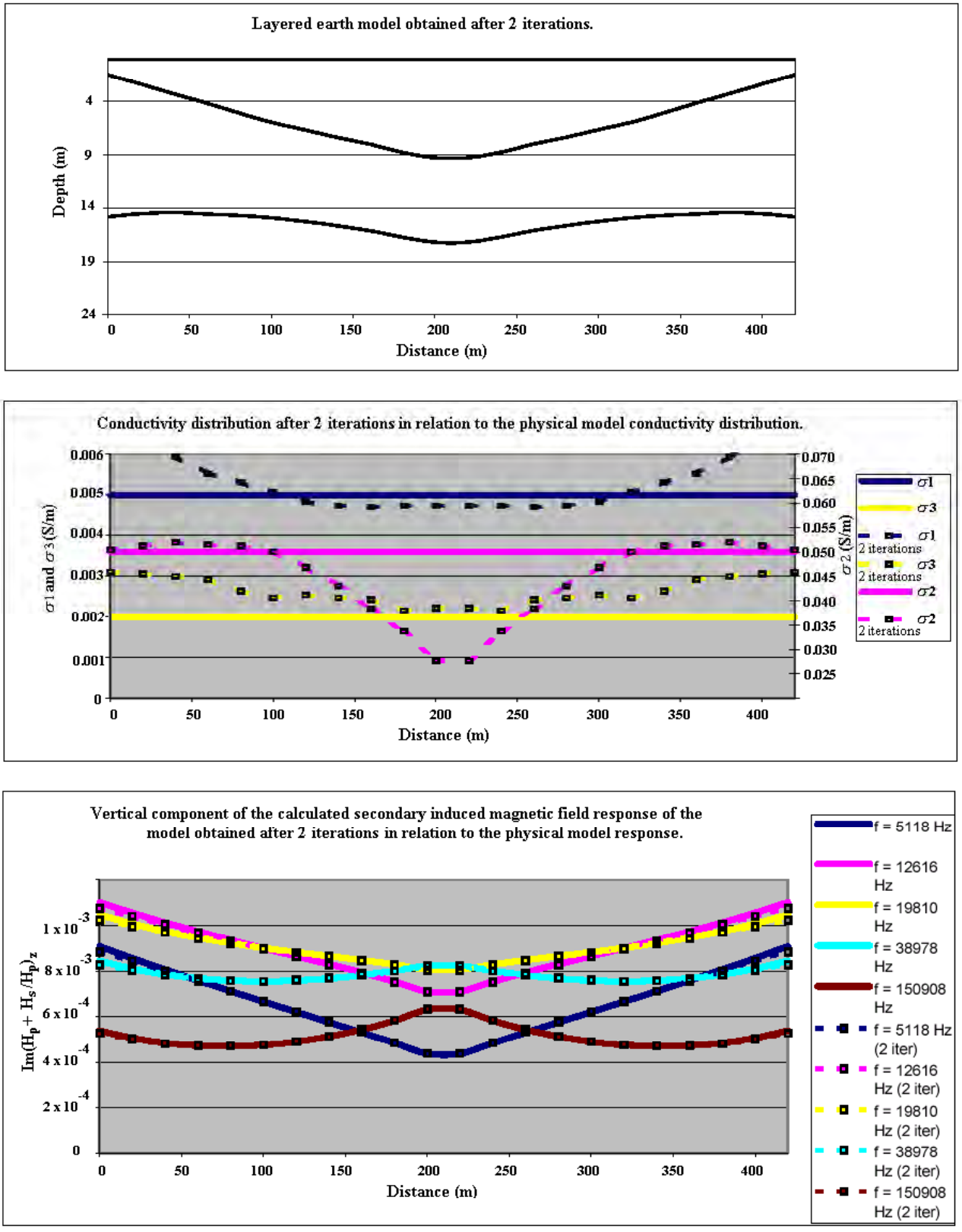

Figure 4.2c. Three-layer model obtained along the profile after 2 iterations.

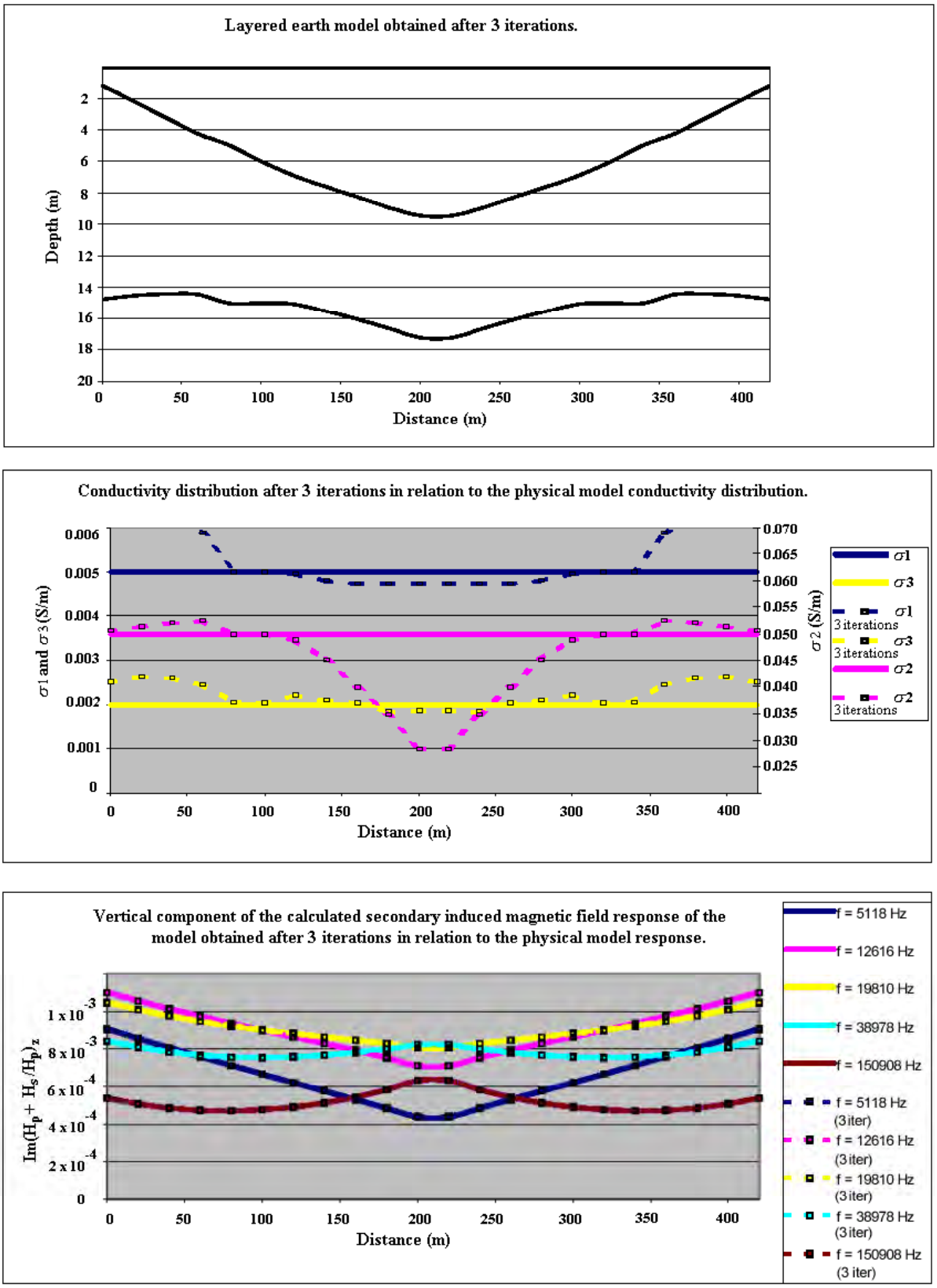

Figure 4.2d. Three-layer model obtained along the profile after 3 iterations.

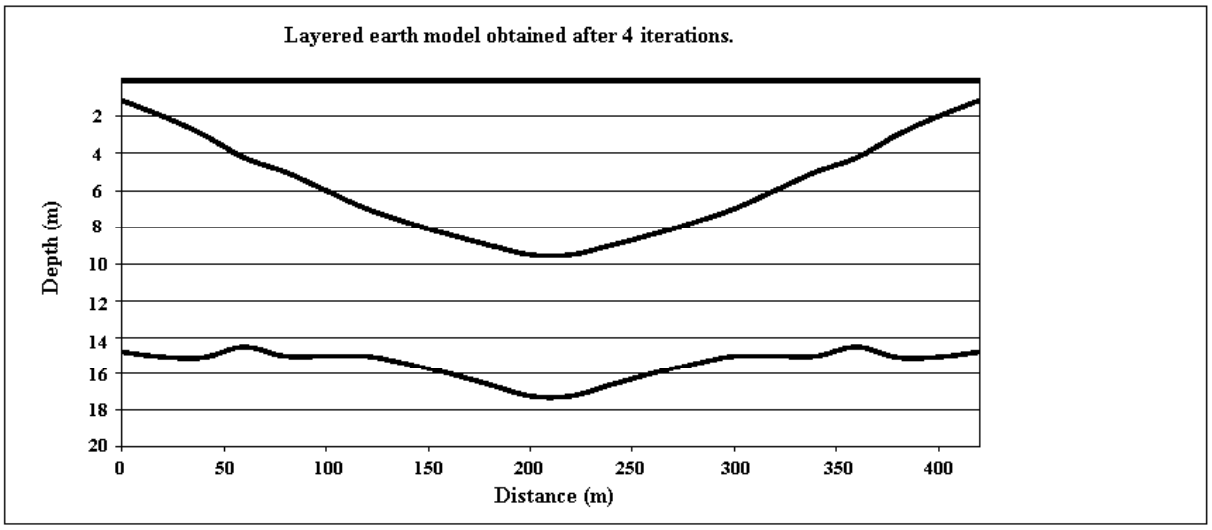

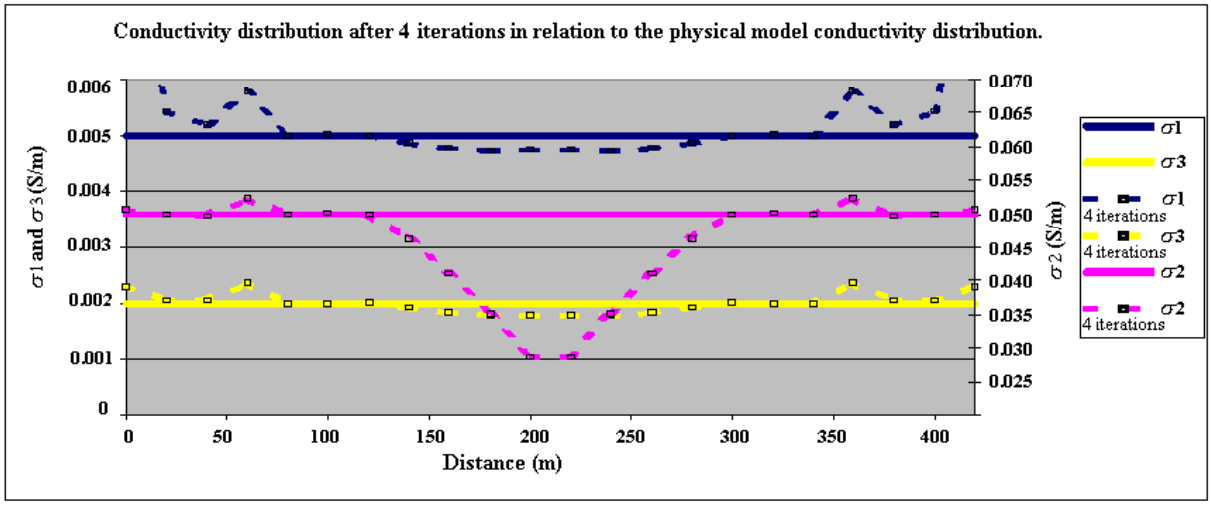

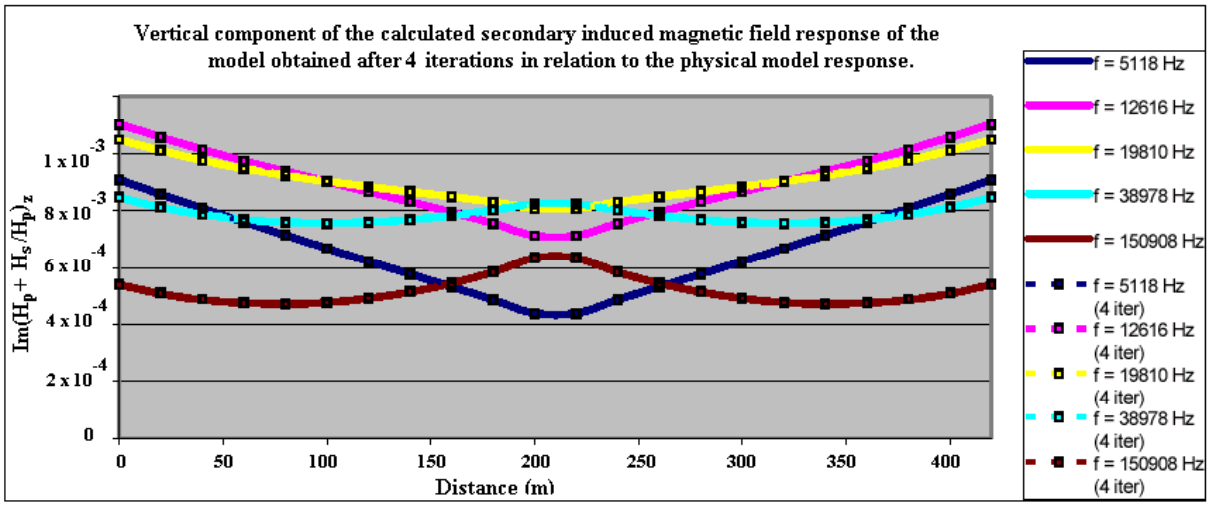

Figure 4.2e. Three-layer model obtained along the profile after 4 iterations.

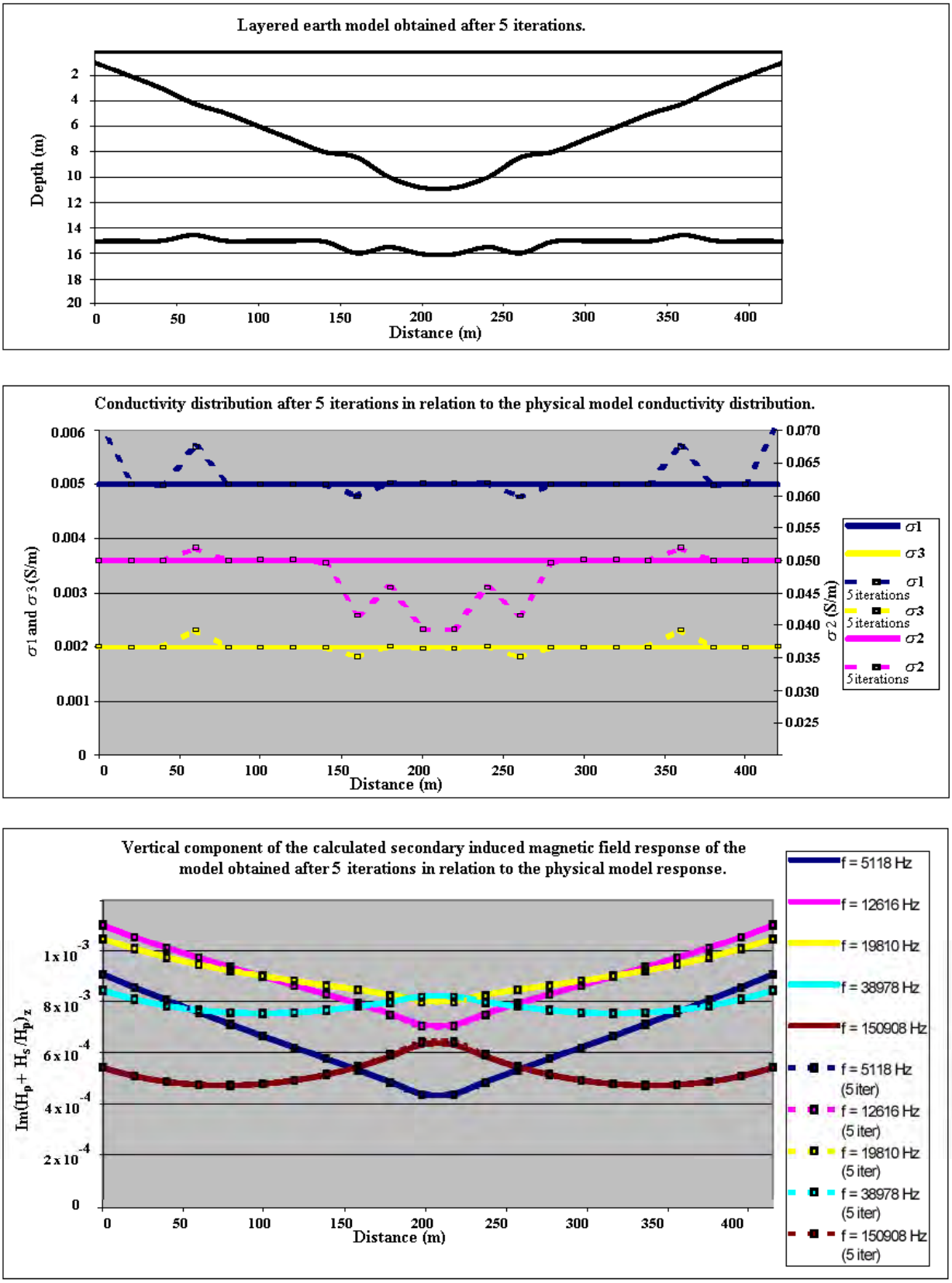

Figure 4.2f. Three-layer model obtained along the profile after 5 iterations.

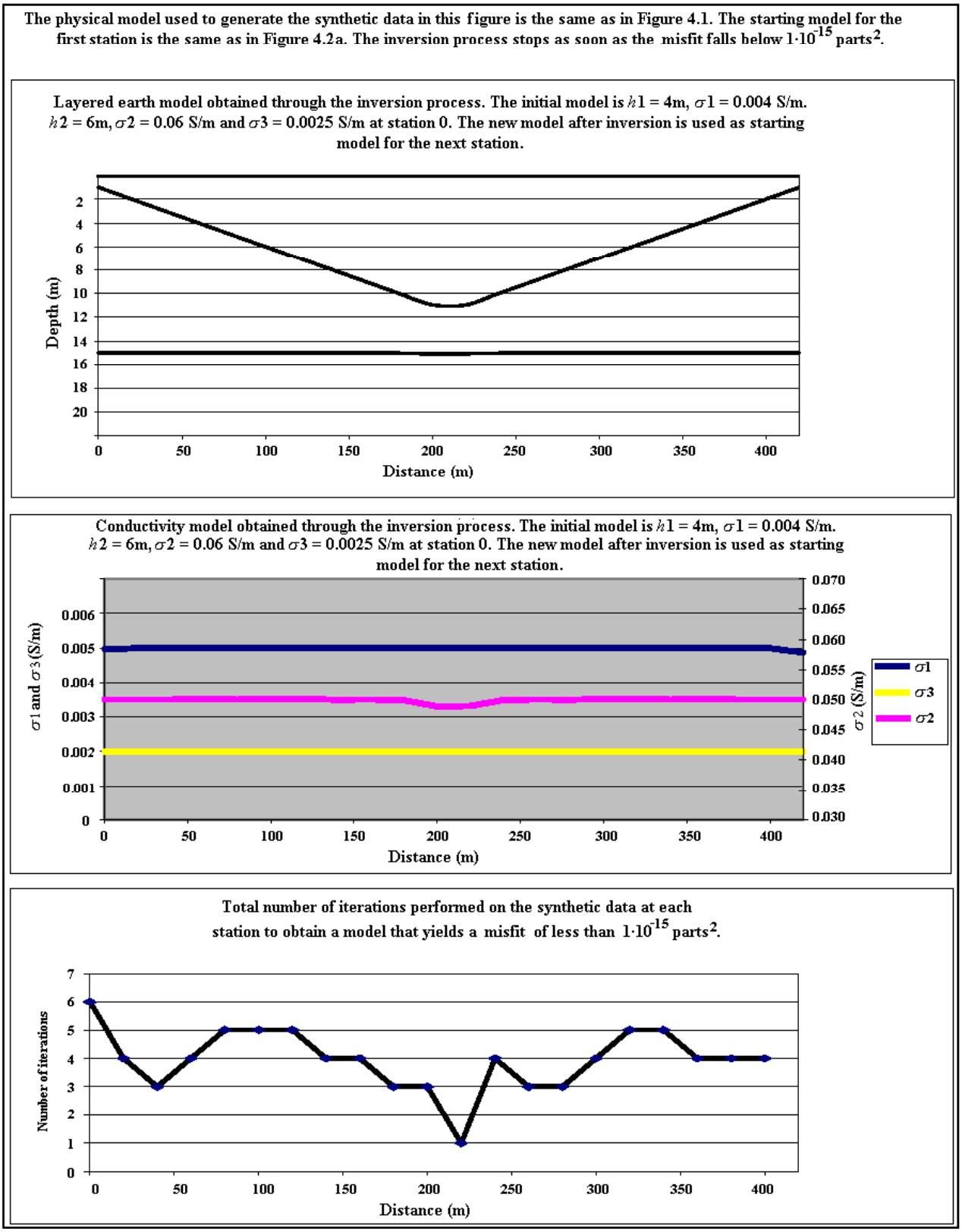

Figure 4.3. Three-layer model obtained through inversion by using the inverted model of the previous station as a starting model for every station along the profile.

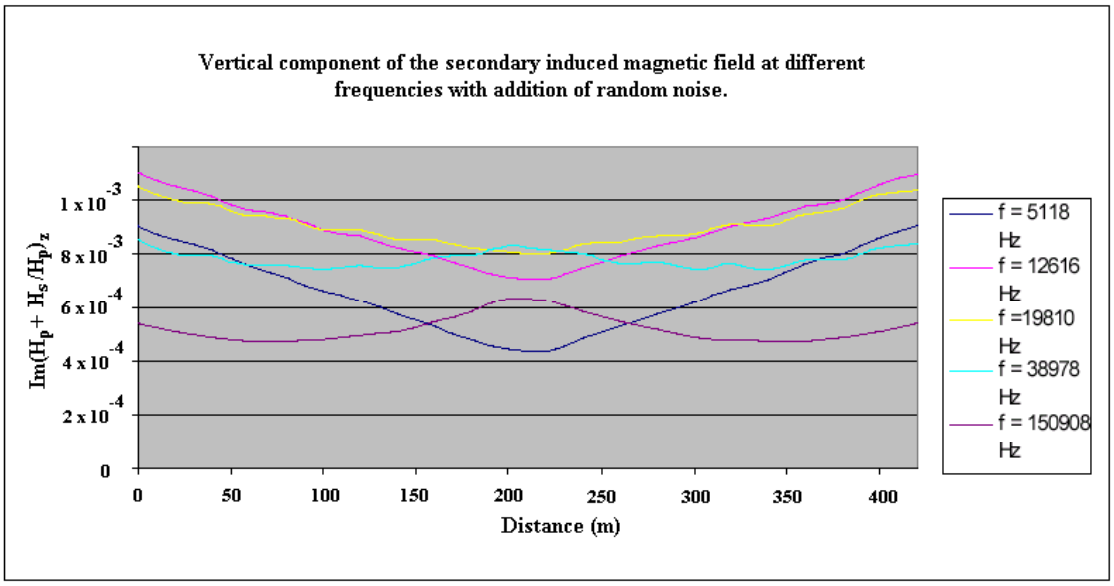

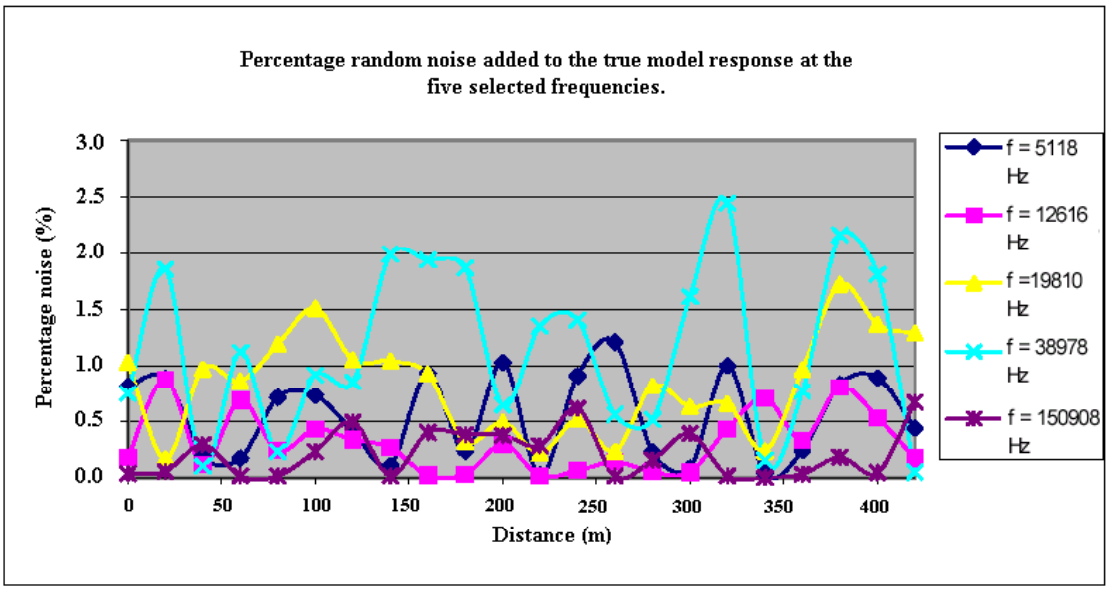

Figure 4.4a. Synthetic data calculated from the physical model in Figure 4.1 with addition of random noise.

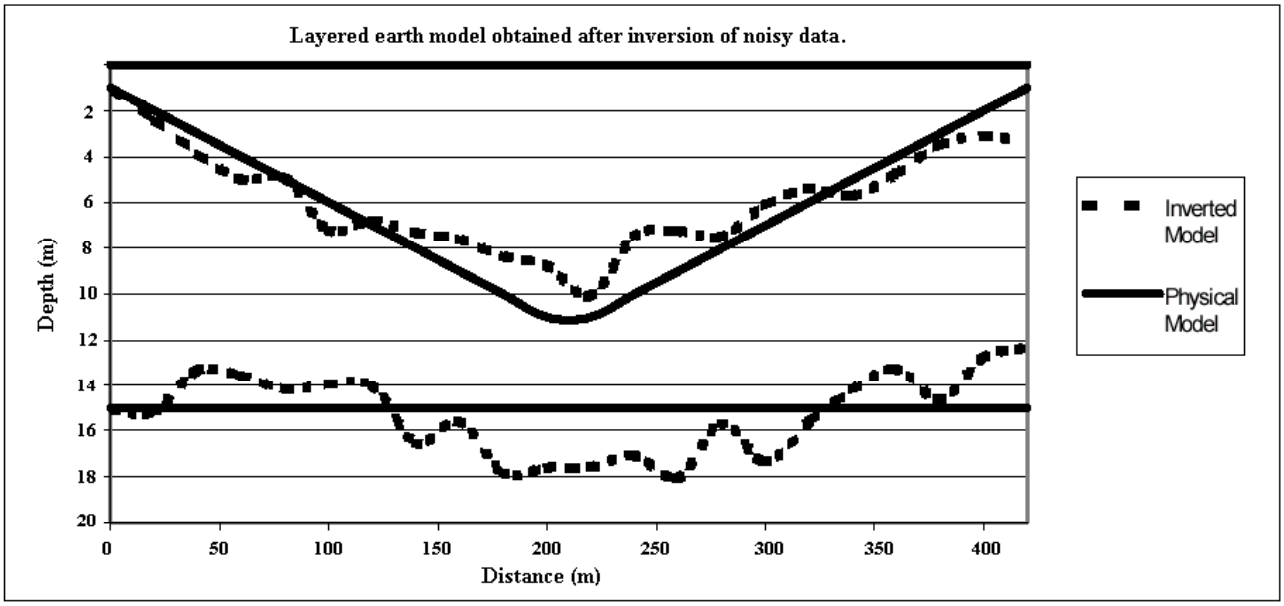

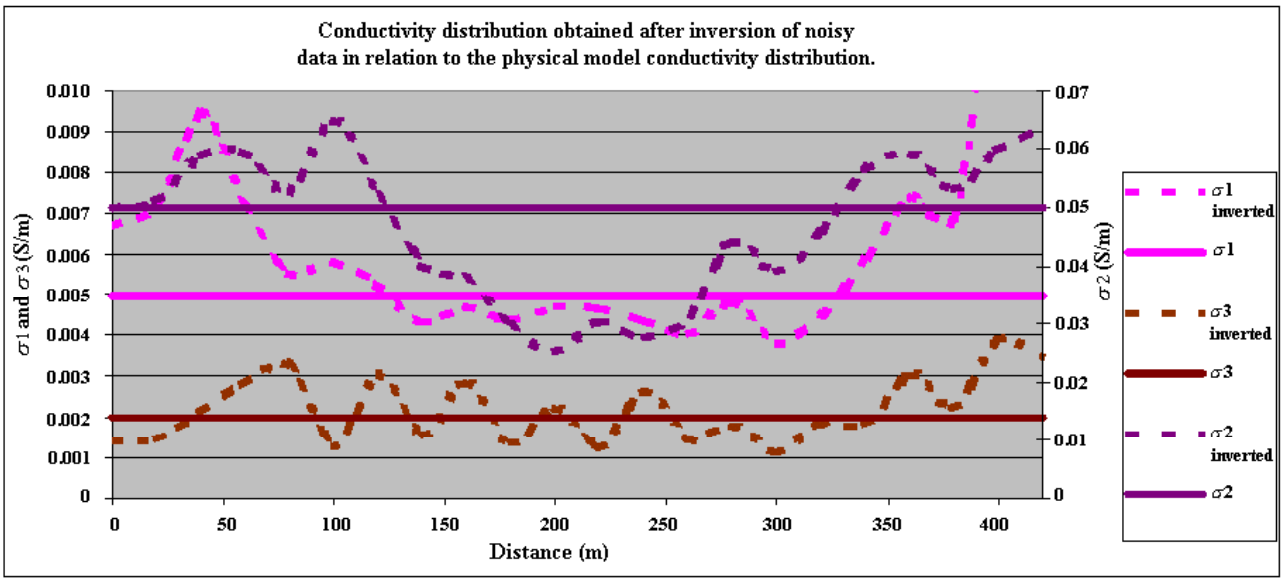

Figure 4.4b. Results obtained after inverting the noisy synthetic data obtained from the physical model in Figure 4.1.

5. CASE STUDY

A DIGHEM V survey was conducted by the University of Pretoria (funded by Fugro Airborne Surveys and the WRC) over the Nebo granites in the Limpopo Province to assess the groundwater potential of the area. The area has been covered simultaneously with airborne magnetics (Figure 5.1). The magnetic data was mainly used in identifying borehole locations for groundwater extraction.

Application of the layered earth algorithm on the airborne EM data can identify whether areas adjacent to linear features, as identified on the magnetic data set, do exhibit positive conductivity anomalies which would indicate conditions possibly favorable to the presence of groundwater. Further, it is important to know the depth to solid granitic bedrock in order to decide on the best possible location for a borehole. If a borehole is drilled in solid unweathered granite, which has a very low permeability, poor yield can be expected with little recharge.

For the DIGHEM V data, the maximum amount of parameters that one can expect to recover are 3 namely, the thickness of the first layer and the conductivity of the first and second layers. This limitation stems from the fact that only three co-planar frequencies are available with the DIGHEM V system. Because of the sparse frequency distribution a conductivity depth transform was not attempted since this would only have resulted in three discreet conductivity values as a function of depth. The approach that was followed was to introduce a control point every 30 stations. At every control point a halfspace model was obtained with an iterative least squares

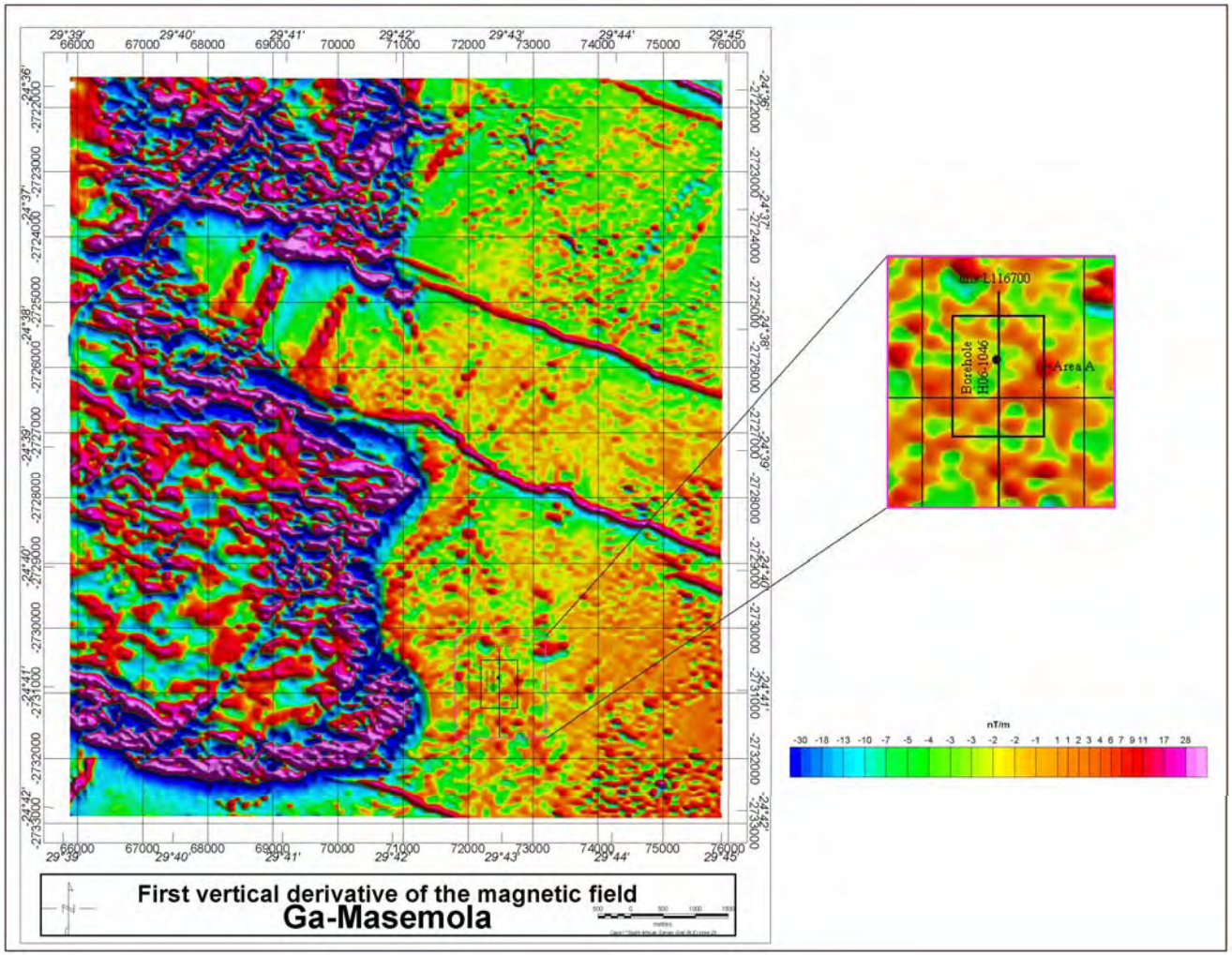

Figure 5.1. Airborne geophysical coverage of the Ga-Masemola area. Developed algorithms have been tested on the DIGHEM V data collected over Area A and along line L116700.

inversion procedure to resemble the observed field data the best. The halfspace conductivity (σ_h) was then used as starting model for both layers and the thickness of the first layer was set at 25m.

The model that was then selected as the solution for the control point was the model that yielded the minimum misfit after 4 iterations. The solution at the control point was subsequently used as starting model for the next 29 stations.

It is very important to note that for the DIGHEM V system the coil separations for the different frequencies are not the same and that the secondary field is normalized with respect to the *x* component of the primary field. If it is assumed that the secondary magnetic field as observed in the coplanar coils is normalized with respect to the *z* component of the primary field, erroneously resistivities will be obtained after inversion. The following table therefore has to be used to prepare the data prior to inversion:

HEM system	Coplanar factor	Coaxial factor	High frequency coplanar factor (if coil separation different from standard)
Aerodat	1	4	
Hummingbird	1	4	
Dighem II pre 1999	2 (uses x normalisation)	4	4 (uses 6.3 rather than 8m separation, x normalisation)
Dighem II post 1998	1	4	2 (uses 6.3 rather than 8m separation)
Geophex UTS, coplanar	1	Not used	

Table 1: Scale factors for different FDEM systems (from ©ENCOM (Emflow) online help files)

Example 1:

Based on the work by Botha et al. (2001) maximum yields for the area under investigation occur in fractured zones in the granite. A northeast striking fracture/fault zone in the granite can be identified on the airborne magnetic data transecting Area A (Figure 5.1). Based on ground follow-up magnetic and EM work Borehole H06-1046 was staked and yielded 3 *l/s* which is above average for this area.

The most adjacent DIGHEM V line to this borehole was processed with the layered earth algorithm. The electromagnetic response for the three co-planar frequencies along line L116700 can be seen in Figure 5.2a. The response calculated from the inverted layered earth model has a very close resemblance to the field data. The physical model obtained after inversion (Figure 5.2b) indicates that the borehole was located at the optimum position along this line. Please note that layer 1 and 2 have different resistivity colour bars. This area of localized deeper weathering and relative more conductive second layer coincides with the fracture zone as seen from the magnetic data. The relative more conductive bedrock associated with this fracture zone is presumed to indicate the presence of moisture while the localized deeper weathering of the first layer would improve recharge.

Drilling results indicated that the deepest water strike was at 20m. The fact that the layered earth inversion algorithm yielded a first layer depth of 30m could be attributed to the presence of a vertical conductivity structure (probably the fracture zone), to the presence of moisture deeper than the

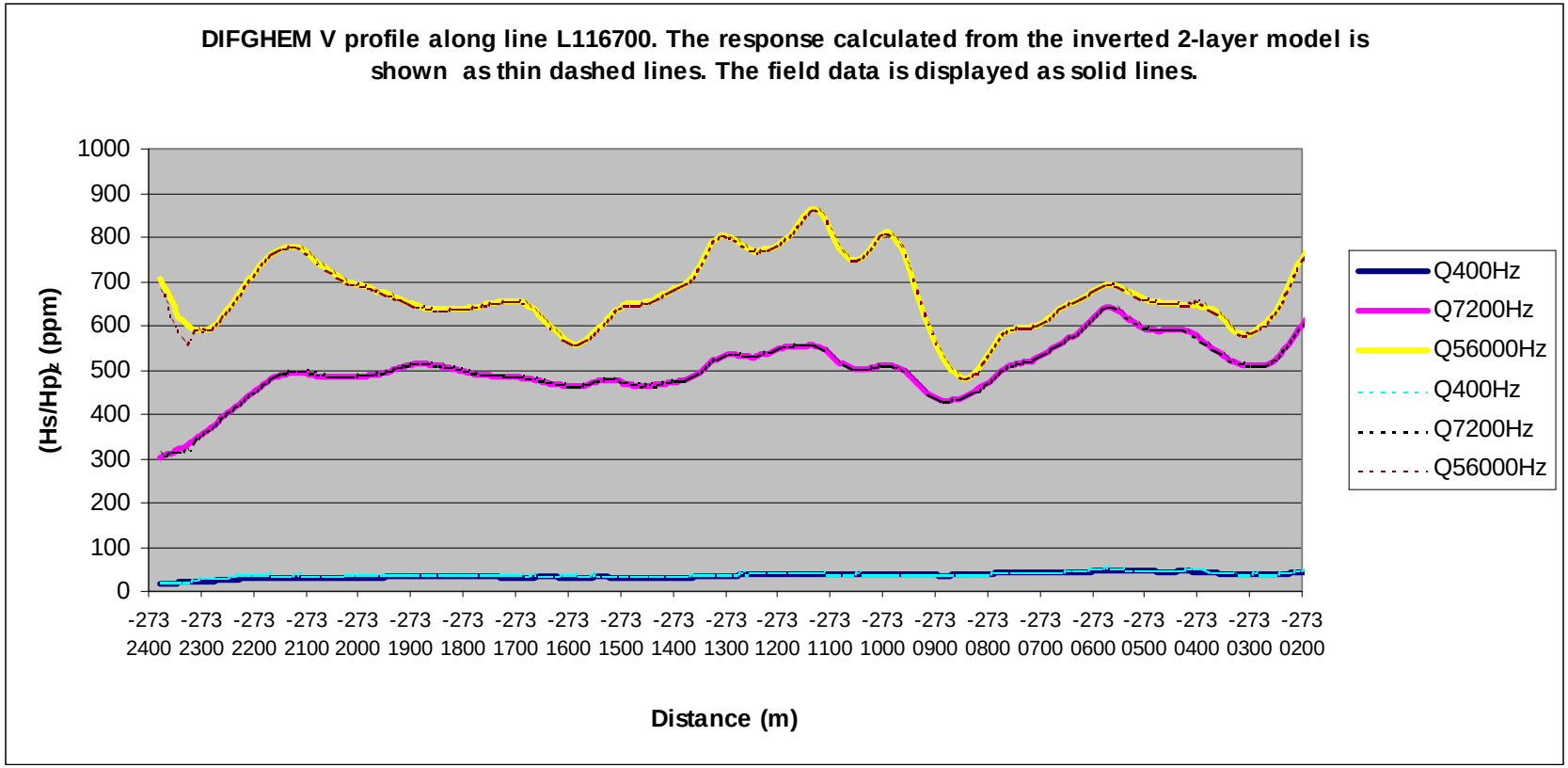

Figure 5.2a. The calculated and observed EM response along line L116700.

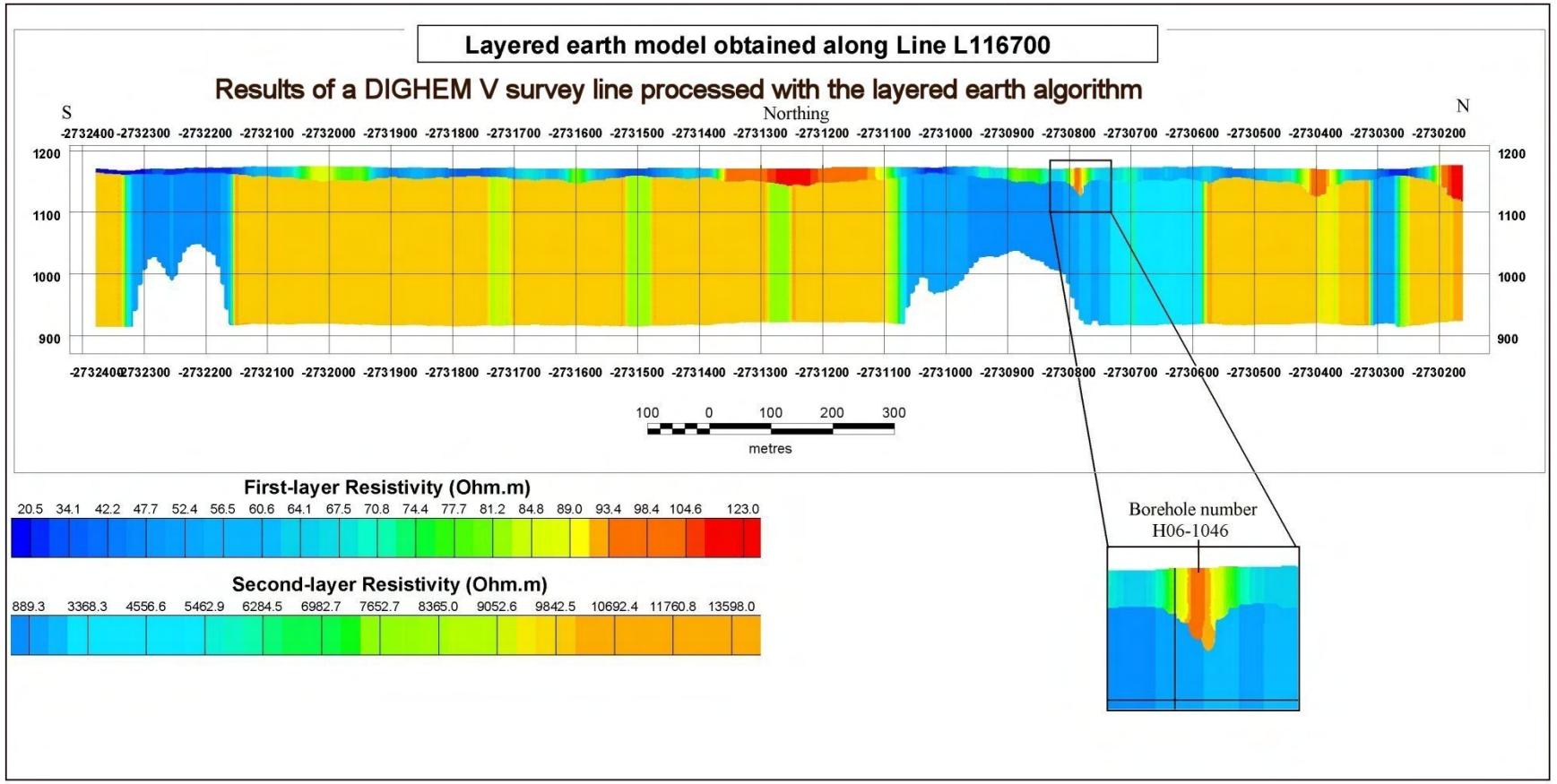

Figure 5.2b. Physical model obtained along line L117600 with the position of borehole H06-1046 shown.

deepest water strike or to a combination thereof. Area A has been deliberately selected for the layered earth inversion routine due to the absence of prominent dike structures visible on the magnetic map.

Although the borehole position was optimal along line L116700 we can now investigate the area surrounding this position to establish if similar or better prospects exist. Further, by having a 2 dimensional model one can get an idea of the structural influences on groundwater movement.

Example 2:

Area A was subsequently processed with the layered earth algorithm. Three figures were prepared from the inversion results. Figure 5.3a shows the depth to bedrock (i.e. the depth at which a significant resistivity contrast occurs between the first and the second layer). Figure 5.3b consists of the first layer resistivity contour map draped over the "bedrock" relief. In Figure 5.3c the second layer resistivity contour map is draped over the "bedrock" relief.

The location of borehole H 06-1046 is shown in Figure 5.3a. It is apparent that the borehole is located in relative thick overburden. The thick overburden at this location forms part of a trough extending in a SE-NW direction. Although a relative thick overburden is implied by the results, high second layer resistivities in the northern and southeastern part of this trough does not present a very good prospect for groundwater reserves. A localized deeply weather zone situated at X 72300, Y -273100 presents a much better prospect. Relative high conductivities in the second layer

implies the presence of moisture which is necessary for recharging the localized aquiver.

Detecting the optimum location for a borehole in a region where highly variable geohydrological conditions exists necessitates detailed investigation. The detailed processing of airborne EM data prior to undertaking a ground follow-up will ensure the identification and demarcation of all viable targets for further investigation.

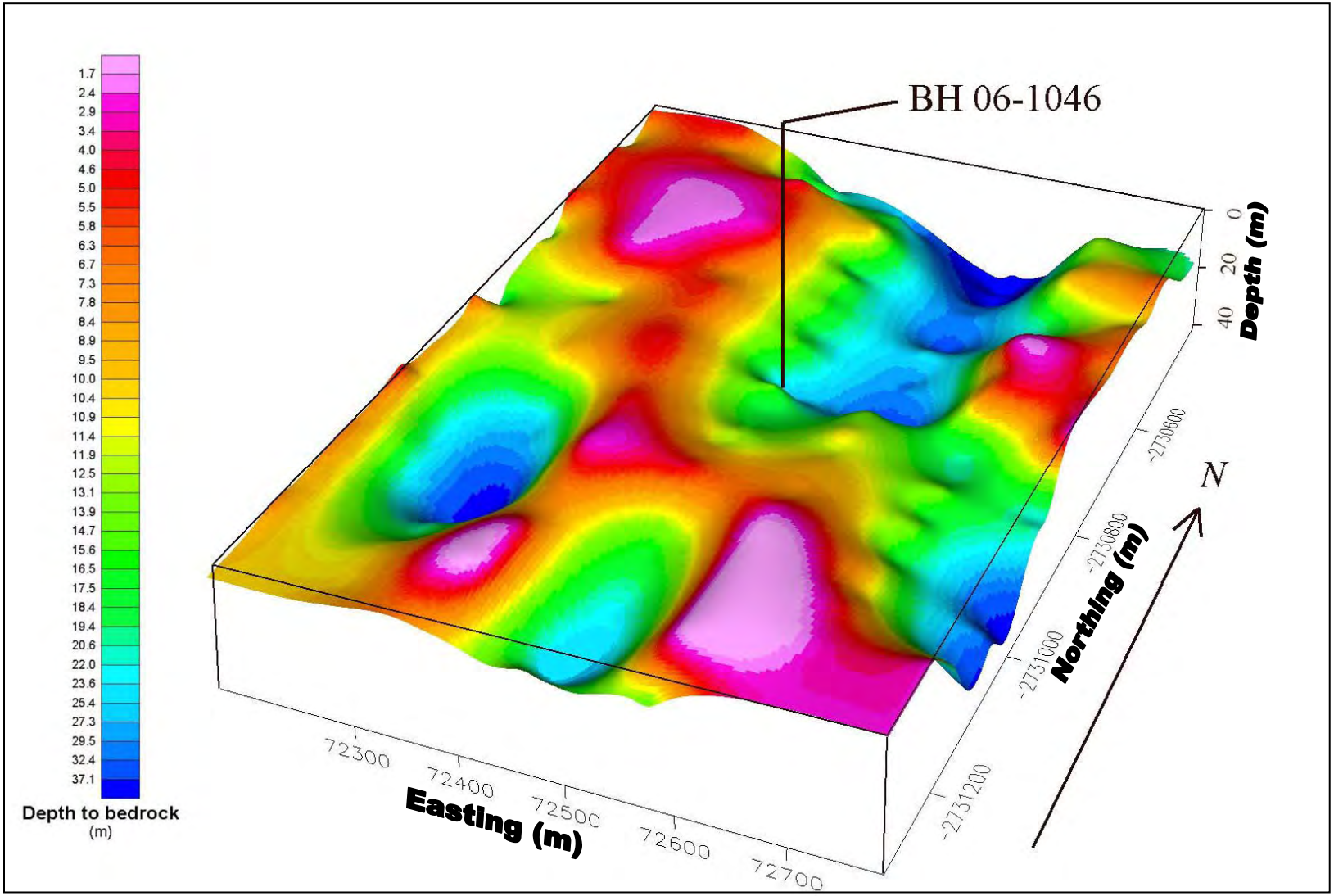

Figure 5.3a. Depth to bedrock map derived from the DIGHEM V data for Area A (Location shown in Figure 5.1).

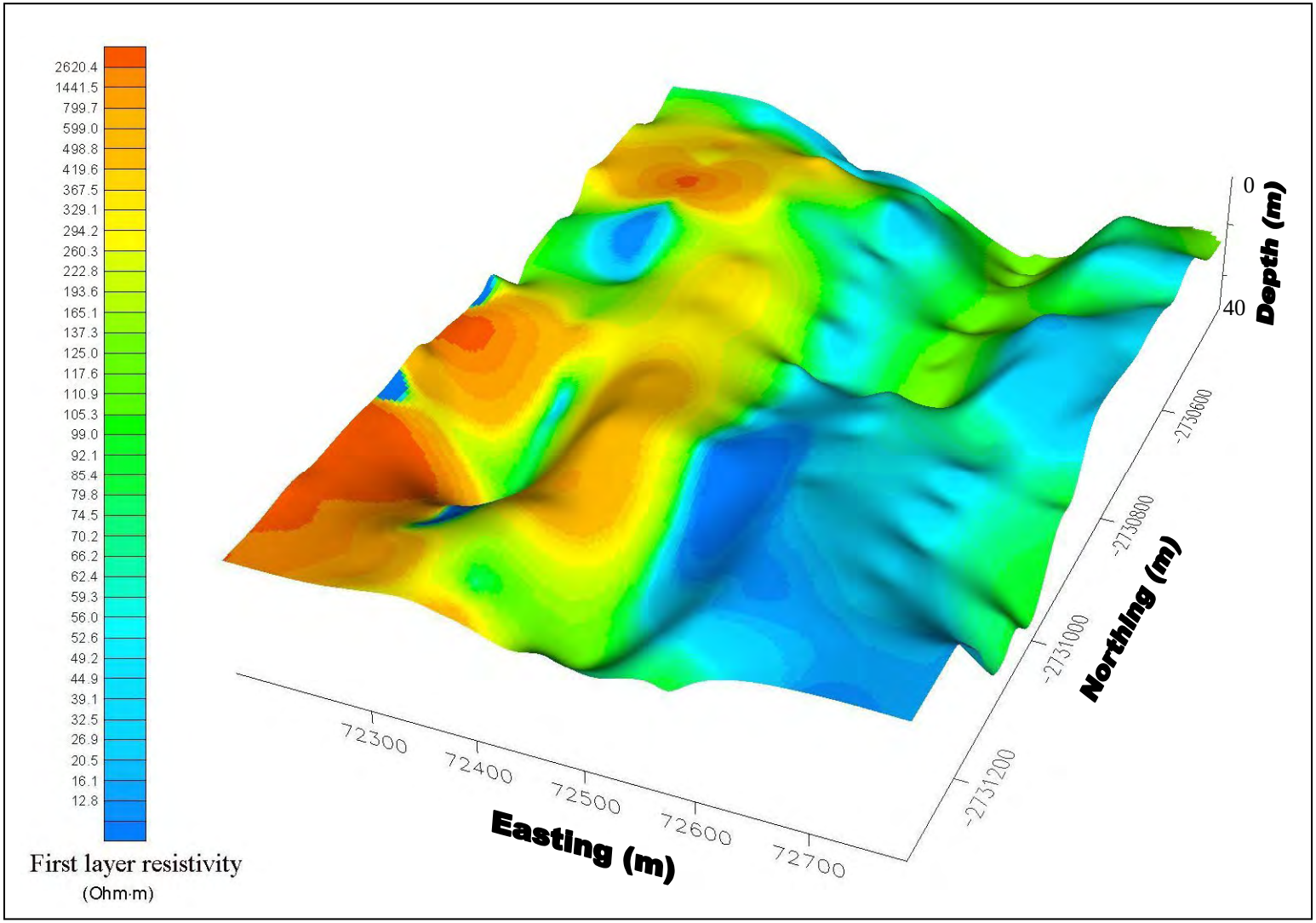

Figure 5.3b. Overburden resistivity distribution draped over the depth to bedrock relief.

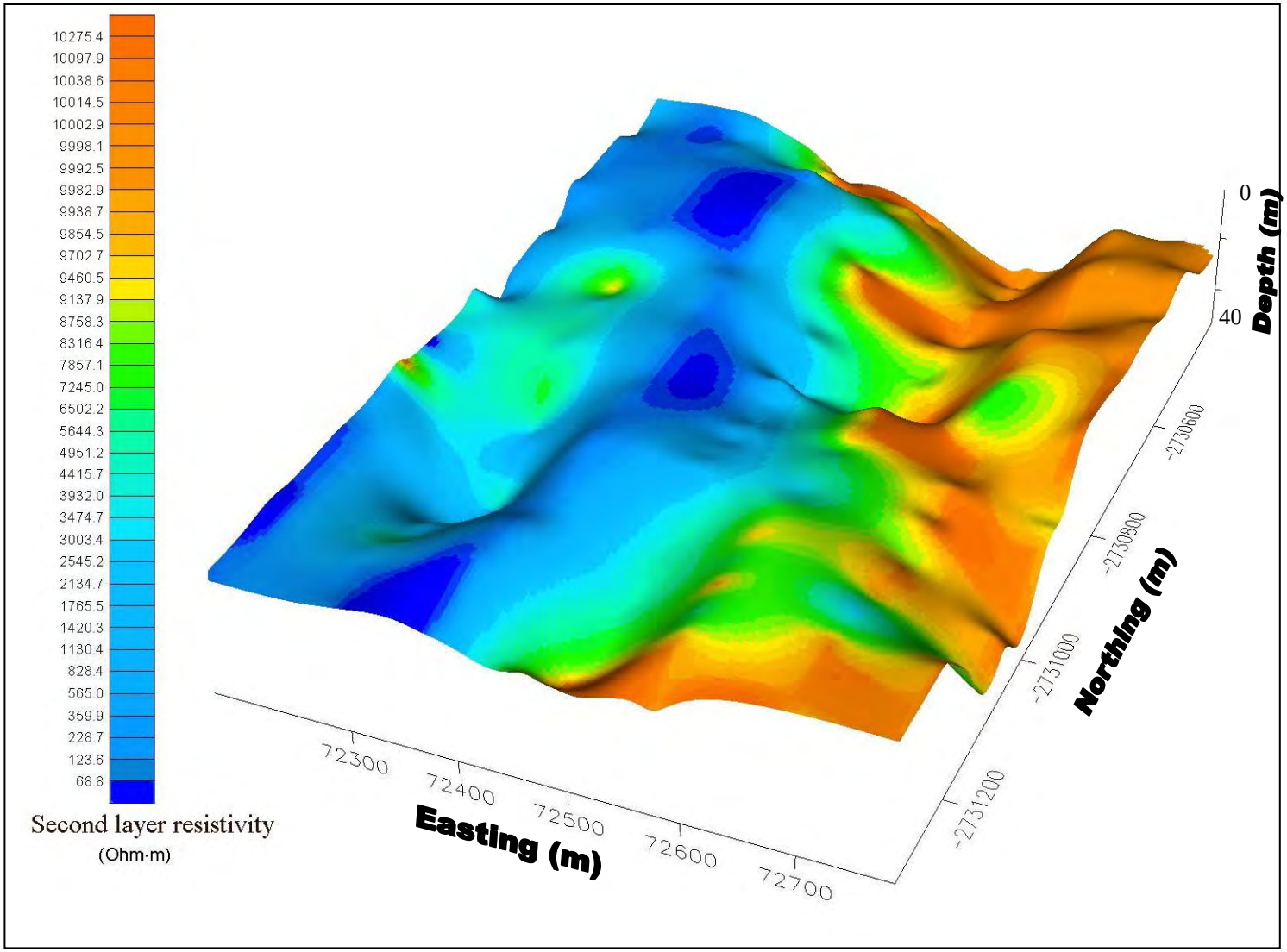

Figure 5.3c. Second layer conductivity distribution draped over the depth to bedrock relief.

6. CONCLUSIONS

Although imaging methods provide a fast approximate image of subsurface conductivity distribution, faster PC's have made the automatic full 1D non-linear damped least-squares inversion of field data possible.

Approximate inversion techniques developed by Sengpiel (1988) and Huang and Fraser (1996) among others have proved to be very useful in obtaining an image of subsurface conductivity distribution, in a relative short time. The main shortcoming of these techniques however is that one can only obtain as many values of conductivity versus depth as there are frequencies present in the data.

Processing DIGHEM V data implies that one only has three co-planar frequencies available. In order to recover as much information as possible from the data we need to minimize the error between the field data and the calculated model response in a least squares sense. Analysis of the partial derivatives used in constructing the Jacobian matrix can provide good indication on the resolvability of physical parameters for the frequencies specific to a platform. Having a good idea of resolvability enables one to have a more realistic view on what output can be expected from the inversion process.

The algorithms tested on the DIGHEM V data have proved to work very well in resolving three parameters namely: depth to bedrock, overburden resistivity and bedrock resistivity.

Equivalence and ambiguity always plays a role in automatic geophysical interpretations. The Council for Geoscience have an in-house developed 3D compact volume joint inversion package for magnetic and gravity data. Future development can focus on incorporating the developed algorithms into this routine to yield a compact volume joint inversion of magnetics, gravity and electromagnetics.

7. REFERENCES

Abramowitz, M and Stegun, I.A., 1964. Handbook of Mathematical functions: Dover Publ., Inc.

Anderson, W.L., 1979. Numerical integration of related Hankel transforms of order 0 and 1 by adaptive filtering: Geophysics, 44, 1287-1305.

Botha, W.J., Combrinck, M., Botha, F.S., and van Rooy, J.L., 2001. An integrated multidisciplinary geophysical approach to groundwater exploration in the Nebo granite, Northern Province: Water Research Commission Report No. 862/1/01, South Africa.

Christensen, N.B., 2002. A generic 1-D imaging method for transient electromagnetic data: Geophysics **67**, 438 – 447.

Christiansen, A.V. and Christensen, N.B., 2003. A quantitative appraisal of airborne and ground-based transient electromagnetic (TEM) measurements in Denmark: Geophysics, **68**, 523 – 534.

Frischknecht, F.C., 1967. Fields about an oscillating magnetic dipole over a two-layered earth, and application to ground and airborne electromagnetic surveys: Quarterly of the Colorado School of Mines, Vol. **62** number 1.

Huang, H., and Fraser, D.C., 1996. The differential parameter method for multifrequency airborne resistivity mapping: Geophysics **61**, 100-109.

Huang, H., and Fraser, D.C., 2003. Inversion of helicopter electromagnetic data to a magnetic conductive layered earth: Geophysics **68**, 1211-1223.

Jupp, D.L., and Vozoff, K., 1975. Stable iterative methods for the inversion of geophysical data: Geophys. J. Roy. Astr. Soc., **42**, 67 – 72.

Kaufman, A. A., and Keller, G.V., 1983. Frequency and transient soundings: Elsevier Science Publ., Inc.

Keller, G.V., and Friscknecht, F.C., 1966. Electrical Methods in Geophysical Prospecting, International Series of Monographs in Electromagnetic Waves Volume 10: Pergamon Press, 278-410.

Lines, L.R., and Treitel, S., 1984. Review of least-squares inversion and its application to geophysical problems: Geoph. Prosp., **32**, 159 – 186.

Macnae, J.C., and Lamontagne, Y., 1987. Imaging quasi-layered conductive structures by simple processing of transient electromagnetic data: Geophysics, **52**, 545 – 554.

Macnae, J.C., Smith, R., Polzer, B.D., Lamontagne, Y., and Klinkert, P.S., 1991. Conductivity-depth imaging of airborne electromagnetic step-response data: Geophysics, **56**, 102-114.

Marquardt, D.W., 1963. An algorithm for least-squares estimation of non-linear parameters, *J. SIAM*, **11**, 431 – 441.

Polzer, B.D., 1985. Interpretation of inductive transient magnetic sounding data: Res. In Appl. Geophys., **36**, University of Toronto.

Sengpiel, K.P. and Siemon, B., 2000. Advanced inversion methods for airborne electromagnetic exploration: Geophysics, **65**, 1983-1992.

Sengpiel, K.P., 1988. Approximate inversion of airborne EM data from a multi-layered ground: Geophys. Prosp., **36** ,446 –459.

Sidorov, V.A. and Tikshaev, V.V., 1970. Interpretation of TDEM curves in "Razvedochnaya geofizika **42**" (in Russian).

Smith, R.S., Edwards, R.N., and Buselli. G., 1994. An automatic technique for presentation of coincident-loop, impulse response, transient electromagnetic data: Geophysics, **59**, 1542-1550.

Stolz, E., and Macnae, J., 1998. Evaluating EM waveforms by singular-value decomposition of exponential bases functions: Geophysics, **63**, 64 - 74.

Telford, W.M., Geldart, L.P., and Sheriff, R.E. (1990) Applied Geophysics, 2nd ed: *Cambridge Univ. Press*, 308-309.

Ward, S.H., and Hohmann, G.W., 1988. Electromagnetic theory for geophysical applications: in Nabighian, M. N., Ed., Electromagnetic

Methods in Applied Geophysics, Society of Exploration Geophysicists, **1**, 130 – 311.

Yi, M.Y., Kim, J.H., and Chung, S.H., 2003. Enhancing the resolving power of least-squares inversion with active constraint balancing: Geophysics, **68**, 931 – 941.

APPENDIX A

Program inverting for a 2-layered earth (h1, $\sigma 1$, $\sigma 2$) using damped least squares inversion with SVD. The program uses (Hs/Hp) where Hs is the z component of the secondary induced magnetic field detected by the EM receiver above the horisontally layered earth and Hp is the z component of the primary field. The program can accomodate any system geometry (i.e. height of Tx, height of Rx, dipole separation). This program is constructed to invert observations at a single location to a 2-layer earth. Synthetic data from Huang and Fraser (1996) is used to test the algorithm.

$$\mu 0 := 4\pi \cdot 10^{-7}$$

$$k0 := 0$$

Forward calculation starts here

****

$$k1(\sigma 1, \omega) := (i \cdot \omega \cdot \mu 0 \cdot \sigma 1)^{\frac{1}{2}}$$

$$k2(\sigma 2, \omega) := (i \cdot \omega \cdot \mu 0 \cdot \sigma 2)^{\frac{1}{2}}$$

$$Y2(\sigma 2, \omega, \lambda) := \left(\lambda^2 + k2(\sigma 2, \omega)^2\right)^{\frac{1}{2}}$$

$$Y'2(\sigma 2, \omega, \lambda) := \left(\lambda^2 + k2(\sigma 2, \omega)^2\right)^{\frac{1}{2}}$$

$$Y1(\sigma1,\omega,\lambda) := \left(\lambda^2 + k1(\sigma1,\omega)^2\right)^{\frac{1}{2}}$$

$$Y'1(h1,\sigma1,\sigma2,\omega,\lambda) := Y1(\sigma1,\omega,\lambda)\cdot\left[\frac{Y'2(\sigma2,\omega,\lambda) + Y1(\sigma1,\omega,\lambda)\cdot\tanh\left[\left(\lambda^2 + k1(\sigma1,\omega)^2\right)^{\frac{1}{2}}\cdot h1\right]}{Y1(\sigma1,\omega,\lambda) + Y'2(\sigma2,\omega,\lambda)\cdot\tanh\left[\left(\lambda^2 + k1(\sigma1,\omega)^2\right)^{\frac{1}{2}}\cdot h1\right]}\right]$$

$$Y0(\omega,\lambda) := \left(\lambda^2 + k0^2\right)^{\frac{1}{2}}$$

$$rTE3(h1,\sigma1,\sigma2,\omega,\lambda) := \frac{\left(Y0(\omega,\lambda) - Y'1(h1,\sigma1,\sigma2,\omega,\lambda)\right)}{\left(Y0(\omega,\lambda) + Y'1(h1,\sigma1,\sigma2,\omega,\lambda)\right)}$$

$$IntFunc(h1,\rho,z,H,\sigma1,\sigma2,\omega,\lambda) := \left(rTE3(h1,\sigma1,\sigma2,\omega,\lambda)\right)\cdot e^{Y0(\omega,\lambda)\cdot(z-H)}\cdot\frac{\lambda^3}{Y0(\omega,\lambda)}\cdot J0(\lambda\cdot\rho)$$

Forward calculation stops here

****

Calculation of partial derivatives starts here

****

First we calculate partial derivatives with respect to parameters in the first layer.

The only parameters that we need to consider is σ1 and h1

First we consider h1

$$Y'1(h1,\sigma1,\sigma2,\omega,\lambda) := Y1(\sigma1,\omega,\lambda)\cdot\left[\frac{Y'2(\sigma2,\omega,\lambda) + Y1(\sigma1,\omega,\lambda)\cdot\tanh\left[\left(\lambda^2 + k1(\sigma1,\omega)^2\right)^{\frac{1}{2}}\cdot h1\right]}{Y1(\sigma1,\omega,\lambda) + Y'2(\sigma2,\omega,\lambda)\cdot\tanh\left[\left(\lambda^2 + k1(\sigma1,\omega)^2\right)^{\frac{1}{2}}\cdot h1\right]}\right]$$

$$A1(h1,\sigma1,\sigma2,\omega,\lambda) := Y1(\sigma1,\omega,\lambda)\cdot\left[1 - \tanh\left[\left(\lambda^2 + k1(\sigma1,\omega)^2\right)^{\frac{1}{2}}\cdot h1\right]^2\right]\cdot\left(\lambda^2 + k1(\sigma1,\omega)^2\right)^{\frac{1}{2}}$$

$$B1(h1,\sigma1,\sigma2,\omega,\lambda) := Y1(\sigma1,\omega,\lambda) + Y'2(\sigma2,\omega,\lambda)\cdot\tanh\left[\left(\lambda^2 + k1(\sigma1,\omega)^2\right)^{\frac{1}{2}}\cdot h1\right]$$

$$C1(h1,\sigma1,\sigma2,\omega,\lambda) := Y'2(\sigma2,\omega,\lambda)\cdot\left[1 - \tanh\left[\left(\lambda^2 + k1(\sigma1,\omega)^2\right)^{\frac{1}{2}}\cdot h1\right]^2\right]\cdot\left(\lambda^2 + k1(\sigma1,\omega)^2\right)^{\frac{1}{2}}$$

$$D1(h1,\sigma1,\sigma2,\omega,\lambda) := Y'2(\sigma2,\omega,\lambda) + Y1(\sigma1,\omega,\lambda)\cdot\tanh\left[\left(\lambda^2 + k1(\sigma1,\omega)^2\right)^{\frac{1}{2}}\cdot h1\right]$$

$$dY'1dh1(h1,\sigma1,\sigma2,\omega,\lambda) := Y1(\sigma1,\omega,\lambda)\cdot\left(\frac{A1(h1,\sigma1,\sigma2,\omega,\lambda)\cdot B1(h1,\sigma1,\sigma2,\omega,\lambda) - D1(h1,\sigma1,\sigma2,\omega,\lambda)\cdot C1(h1,\sigma1,\sigma2,\omega,\lambda)}{B1(h1,\sigma1,\sigma2,\omega,\lambda)^2}\right)$$

$$drTEdh1(h1,\sigma1,\sigma2,\omega,\lambda) := \frac{-2\cdot Y0(\omega,\lambda)}{(Y0(\omega,\lambda) + Y'1(h1,\sigma1,\sigma2,\omega,\lambda))^2}\cdot dY'1dh1(h1,\sigma1,\sigma2,\omega,\lambda)$$

$$IntFunc1(h1,\rho,z,H,\sigma1,\sigma2,\omega,\lambda) := (drTEdh1(h1,\sigma1,\sigma2,\omega,\lambda))\cdot e^{Y0(\omega,\lambda)\cdot(z-H)}\cdot\frac{\lambda^3}{Y0(\omega,\lambda)}\cdot J0(\lambda\cdot\rho)$$

Next we consider $\sigma1$

$$Y'1(h1,\sigma1,\sigma2,\omega,\lambda) := Y1(\sigma1,\omega,\lambda)\cdot\left[\frac{Y'2(\sigma2,\omega,\lambda) + Y1(\sigma1,\omega,\lambda)\cdot\tanh\left[\left(\lambda^2 + k1(\sigma1,\omega)^2\right)^{\frac{1}{2}}\cdot h1\right]}{Y1(\sigma1,\omega,\lambda) + Y'2(\sigma2,\omega,\lambda)\cdot\tanh\left[\left(\lambda^2 + k1(\sigma1,\omega)^2\right)^{\frac{1}{2}}\cdot h1\right]}\right]$$

$$dY1d\sigma1(\sigma1,\omega,\lambda) := \frac{1}{2}\left(\lambda^2 + i\cdot\omega\cdot\mu0\cdot\sigma1\right)^{-0.5}\cdot(i\cdot\omega\cdot\mu0)$$

$$A2(h1,\sigma1,\sigma2,\omega,\lambda) := \left[1 - \tanh\left[\left(\lambda^2 + k1(\sigma1,\omega)^2\right)^{\frac{1}{2}}\cdot h1\right]^2\right]\cdot h1\cdot dY1d\sigma1(\sigma1,\omega,\lambda)$$

$$B2(h1,\sigma1,\sigma2,\omega,\lambda) := Y1(\sigma1,\omega,\lambda)\cdot A2(h1,\sigma1,\sigma2,\omega,\lambda) + dY1d\sigma1(\sigma1,\omega,\lambda)\cdot\tanh\left[\left(\lambda^2 + k1(\sigma1,\omega)^2\right)^{\frac{1}{2}}\cdot h1\right]$$

$$C2(h1,\sigma1,\sigma2,\omega,\lambda) := dY1d\sigma1(\sigma1,\omega,\lambda) + Y'2(\sigma2,\omega,\lambda)\cdot A2(h1,\sigma1,\sigma2,\omega,\lambda)$$

$$D2(h1,\sigma1,\sigma2,\omega,\lambda) := Y'2(\sigma2,\omega,\lambda) + Y1(\sigma1,\omega,\lambda)\cdot\tanh\left[\left(\lambda^2 + k1(\sigma1,\omega)^2\right)^{\frac{1}{2}}\cdot h1\right]$$

$$E2(h1,\sigma1,\sigma2,\omega,\lambda) := Y1(\sigma1,\omega,\lambda) + Y'2(\sigma2,\omega,\lambda)\cdot\tanh\left[\left(\lambda^2 + k1(\sigma1,\omega)^2\right)^{\frac{1}{2}}\cdot h1\right]$$

$$F2(h1,\sigma1,\sigma2,\omega,\lambda) := \frac{B2(h1,\sigma1,\sigma2,\omega,\lambda)\cdot E2(h1,\sigma1,\sigma2,\omega,\lambda) - D2(h1,\sigma1,\sigma2,\omega,\lambda)\cdot C2(h1,\sigma1,\sigma2,\omega,\lambda)}{E2(h1,\sigma1,\sigma2,\omega,\lambda)^2}$$

$$dY'1d\sigma1(h1,\sigma1,\sigma2,\omega,\lambda) := Y1(\sigma1,\omega,\lambda)\cdot F2(h1,\sigma1,\sigma2,\omega,\lambda) + dY1d\sigma1(\sigma1,\omega,\lambda)\cdot\frac{D2(h1,\sigma1,\sigma2,\omega,\lambda)}{E2(h1,\sigma1,\sigma2,\omega,\lambda)}$$

$$drTEd\sigma1(h1,\sigma1,\sigma2,\omega,\lambda) := \frac{-2\cdot Y0(\omega,\lambda)}{\left(Y0(\omega,\lambda) + Y'1(h1,\sigma1,\sigma2,\omega,\lambda)\right)^2}\cdot dY'1d\sigma1(h1,\sigma1,\sigma2,\omega,\lambda)$$

$$IntFunc2(h1,\rho,z,H,\sigma1,\sigma2,\omega,\lambda) := \left(drTEd\sigma1(h1,\sigma1,\sigma2,\omega,\lambda)\right)\cdot e^{Y0(\omega,\lambda)\cdot(z-H)}\cdot\frac{\lambda^3}{Y0(\omega,\lambda)}\cdot J0(\lambda\cdot\rho)$$

We now determine the partial derivatives for the only resolvable parameter in the second layer namely $\sigma 2$

$$Y'2(\sigma 2,\omega,\lambda) := \left(\lambda^2 + k2(\sigma 2,\omega)^2\right)^{\frac{1}{2}}$$

$$dY'2d\sigma 2(\sigma 2,\omega,\lambda) := \frac{1}{2}\left(\lambda^2 + i\cdot\omega\cdot\mu 0\cdot\sigma 2\right)^{-1\cdot\frac{1}{2}}\cdot(i\cdot\omega\cdot\mu 0)$$

$$Y'1Y'2(h1,\sigma 1,\sigma 2,\omega,\lambda) := \frac{(Y1(\sigma 1,\omega,\lambda))^2\cdot\left[1 - \tanh\left[\left(\lambda^2 + k1(\sigma 1,\omega)^2\right)^{\frac{1}{2}}\cdot h1\right]^2\right]}{\left[Y1(\sigma 1,\omega,\lambda) + Y'2(\sigma 2,\omega,\lambda)\cdot\tanh\left[\left(\lambda^2 + k1(\sigma 1,\omega)^2\right)^{\frac{1}{2}}\cdot h1\right]\right]^2}$$

$$drTEd\sigma 2(h1,\sigma 1,\sigma 2,\omega,\lambda) := \frac{-2\cdot Y0(\omega,\lambda)}{(Y0(\omega,\lambda) + Y'1(h1,\sigma 1,\sigma 2,\omega,\lambda))^2}\cdot(Y'1Y'2(h1,\sigma 1,\sigma 2,\omega,\lambda)\cdot dY'2d\sigma 2(\sigma 2,\omega,\lambda))$$

$$IntFunc3(h1,\rho,z,H,\sigma 1,\sigma 2,\omega,\lambda) := (drTEd\sigma 2(h1,\sigma 1,\sigma 2,\omega,\lambda))\cdot e^{Y0(\omega,\lambda)\cdot(z-H)}\cdot\frac{\lambda^3}{Y0(\omega,\lambda)}\cdot J0(\lambda\cdot\rho)$$

Calculation of partial derivatives stops here

****

The z component of the primary field is given by

****

$$zz(z,H) := -1\cdot(H+z)$$

$$Hp(z,H,\rho) := \frac{2\cdot(zz(z,H))^2 - \rho^2}{\left[\rho^2 + (zz(z,H))^2\right]^{\frac{5}{2}}}$$

The forward calculation is now given by

****

$$Hs(h1,\rho,z,H,\sigma1,\sigma2,\omega) := \int_0^{0.3} IntFunc(h1,\rho,z,H,\sigma1,\sigma2,\omega,\lambda)\,d\lambda$$

$$ZZ0(h1,\rho,z,H,\sigma1,\sigma2,\omega) := \frac{Hs(h1,\rho,z,H,\sigma1,\sigma2,\omega)}{Hp(z,H,\rho)}$$

The partial derivatives are given by

****

$$dHsdh1(h1,\rho,z,H,\sigma1,\sigma2,\omega) := \int_0^{0.3} IntFunc1(h1,\rho,z,H,\sigma1,\sigma2,\omega,\lambda)\,d\lambda$$

$$dZZ0dh1(h1,\rho,z,H,\sigma1,\sigma2,\omega) := \frac{dHsdh1(h1,\rho,z,H,\sigma1,\sigma2,\omega)}{Hp(z,H,\rho)}$$

$$dHsd\sigma1(h1,\rho,z,H,\sigma1,\sigma2,\omega) := \int_0^{0.3} IntFunc2(h1,\rho,z,H,\sigma1,\sigma2,\omega,\lambda)\, d\lambda$$

$$dZZ0d\sigma1(h1,\rho,z,H,\sigma1,\sigma2,\omega) := \frac{dHsd\sigma1(h1,\rho,z,H,\sigma1,\sigma2,\omega)}{Hp(z,H,\rho)}$$

$$dHsd\sigma2(h1,\rho,z,H,\sigma1,\sigma2,\omega) := \int_0^{0.3} IntFunc3(h1,\rho,z,H,\sigma1,\sigma2,\omega,\lambda)\, d\lambda$$

$$dZZ0d\sigma2(h1,\rho,z,H,\sigma1,\sigma2,\omega) := \frac{dHsd\sigma2(h1,\rho,z,H,\sigma1,\sigma2,\omega)}{Hp(z,H,\rho)}$$

****

System specs

$H := 30$

$z := -30$

$\rho1 := 8$

$\rho2 := 8$

****

$$f := \begin{pmatrix} 57600 \\ 14400 \\ 1800 \end{pmatrix}$$ Frequencies where field observations are made

$\omega 1 := 2 \cdot \pi \cdot f_0$

$\omega 2 := 2 \cdot \pi \cdot f_1$

$\omega 3 := 2 \cdot \pi \cdot f_2$

The synthetic model is a 2-layer model. The ppm amplitudes from Huang and Fraser (1996) must be multiplied by 2 before the inversion. This is because they normalized their secondary magnetic field with respect to the x component of the primary field and the mathematics in this algorithm assumes normalization with respect to the z component.

$$dobsv := \begin{pmatrix} 1423 \\ 894.6 \\ 160.4 \end{pmatrix}$$

Synthetic data that is observed when h1 = 10m, $\sigma 1$ = 0.02 S/m and $\sigma 2$ S/m = 0.001.

we can now construct the Jacobian matrix

****

$$J(h1, \sigma 1, \sigma 2) := \begin{pmatrix} h1 \cdot Im(dZZ0dh1(h1, \rho 1, z, H, \sigma 1, \sigma 2, \omega 1)) & \sigma 1 \cdot Im(dZZ0d\sigma 1(h1, \rho 1, z, H, \sigma 1, \sigma 2, \omega 1)) & \sigma 2 \cdot Im(dZZ0d\sigma 2(h1, \rho 1, z, H, \sigma 1, \sigma 2, \omega 1)) \\ h1 \cdot Im(dZZ0dh1(h1, \rho 1, z, H, \sigma 1, \sigma 2, \omega 2)) & \sigma 1 \cdot Im(dZZ0d\sigma 1(h1, \rho 1, z, H, \sigma 1, \sigma 2, \omega 2)) & \sigma 2 \cdot Im(dZZ0d\sigma 2(h1, \rho 1, z, H, \sigma 1, \sigma 2, \omega 2)) \\ h1 \cdot Im(dZZ0dh1(h1, \rho 2, z, H, \sigma 1, \sigma 2, \omega 3)) & \sigma 1 \cdot Im(dZZ0d\sigma 1(h1, \rho 2, z, H, \sigma 1, \sigma 2, \omega 3)) & \sigma 2 \cdot Im(dZZ0d\sigma 2(h1, \rho 2, z, H, \sigma 1, \sigma 2, \omega 3)) \end{pmatrix}$$

$$F(h1,\sigma1,\sigma2) := \begin{pmatrix} \mathrm{Im}(ZZ0(h1,\rho1,z,H,\sigma1,\sigma2,\omega1)) \\ \mathrm{Im}(ZZ0(h1,\rho1,z,H,\sigma1,\sigma2,\omega2)) \\ \mathrm{Im}(ZZ0(h1,\rho2,z,H,\sigma1,\sigma2,\omega3)) \end{pmatrix} \qquad Ftest(h1,\sigma1,\sigma2) := \begin{pmatrix} \mathrm{Im}(ZZ0(h1,\rho1,z,H,\sigma1,\sigma2,\omega1)) \\ \mathrm{Im}(ZZ0(h1,\rho1,z,H,\sigma1,\sigma2,\omega2)) \\ \mathrm{Im}(ZZ0(h1,\rho2,z,H,\sigma1,\sigma2,\omega3)) \end{pmatrix} \cdot 1000000$$

$$Ftest(10,0.02,0.001) = \begin{pmatrix} 1.422977 \times 10^{3} \\ 894.662186 \\ 160.504036 \end{pmatrix}$$

We now assume that d is the observed data vector and we try to obtain the model parameter vector.
We therefore have to guess an in initial parameter vector p0

$$p0 := \begin{pmatrix} 5 \\ 0.05 \\ 0.005 \end{pmatrix}$$

With the begin parameters h1,σ1,σ2 respectively

$$x0 := \ln(p0)$$

$$h1 := e^{x0_0}$$

$$\sigma1 := e^{x0_1}$$

$$\sigma2 := e^{x0_2}$$

$$\text{Par}(r, \text{stations}) := \text{for } w \in 0..\text{stations}$$

$$x \leftarrow x0$$

$$h1 \leftarrow e^{x0_0}$$

$$\sigma 1 \leftarrow e^{x0_1}$$

$$\sigma 2 \leftarrow e^{x0_2}$$

$$\text{for } t \in 0..2$$

$$d_t \leftarrow \frac{\text{dobsv}_{t,w}}{1000000}$$

$$\text{sum} \leftarrow 0$$

$$\text{sum1} \leftarrow 1$$

$$\text{sum2} \leftarrow 1$$

$$\beta nn \leftarrow 0$$

$$\text{erg} \leftarrow \left(d - F(h1, \sigma 1, \sigma 2)\right)^2$$

$$\text{er1g} \leftarrow \text{erg}_0$$

$$\text{er2g} \leftarrow \text{erg}_1$$

$$\text{er3g} \leftarrow \text{erg}_2$$

$$\text{Misfitg} \leftarrow \frac{\text{er1g} + \text{er2g} + \text{er3g}}{3}$$

$$\text{Model}_{0,0} \leftarrow 0$$

$$\text{Model}_{0,1} \leftarrow h1$$

$$\text{Model}_{0,2} \leftarrow \sigma 1$$

$\text{Model}_{0,3} \leftarrow \sigma 2$

$\text{Model}_{0,4} \leftarrow \text{Misfitg}$

for $i \in 0..r$

$n \leftarrow \text{rows}(J(h1, \sigma 1, \sigma 2))$

$p \leftarrow \text{cols}(J(h1, \sigma 1, \sigma 2))$

$SVD \leftarrow \text{svd}(J(h1, \sigma 1, \sigma 2))$

$s \leftarrow \text{svds}(J(h1, \sigma 1, \sigma 2))$

$\Lambda \leftarrow \text{diag}(s)$

$U \leftarrow \text{submatrix}(SVD, 0, n-1, 0, p-1)$

$V \leftarrow \text{submatrix}(SVD, n, n+p-1, 0, p-1)$

$I \leftarrow \text{identity}(p)$

$deld \leftarrow d - F(h1, \sigma 1, \sigma 2)$

for $M \in 1..10$

$\beta n \leftarrow 1 \cdot 10^{(M \cdot 0.5 - 13)}$

$delp \leftarrow V \cdot \left(\Lambda^2 + \beta n \cdot I\right)^{-1} \cdot \Lambda \cdot ((U))^T \cdot deld$

$xn \leftarrow x + delp$

$h1n \leftarrow e^{xn_0}$

$\sigma 1n \leftarrow e^{xn_1}$

$\sigma 2n \leftarrow e^{xn_2}$

$er \leftarrow (d - F(h1n, \sigma 1n, \sigma 2n))^2$

$er1 \leftarrow er_0$

$er2 \leftarrow er_1$

$er3 \leftarrow er_2$

$Misfitn \leftarrow \frac{er1 + er2 + er3}{n}$

$sum1 \leftarrow Misfitn \quad if \quad Misfitn < sum1$

$\beta nn \leftarrow \beta n \quad if \quad Misfitn = sum1$

$\beta \leftarrow \beta nn$

$delp \leftarrow V \cdot \left(\Lambda^2 + \beta \cdot I\right)^{-1} \cdot \Lambda \cdot [((U))]^T \cdot deld$

$x \leftarrow x + delp$

$h1 \leftarrow e^{x_0}$

$\sigma 1 \leftarrow e^{x_1}$

$\sigma 2 \leftarrow e^{x_2}$

$er \leftarrow \left(d - F(h1, \sigma 1, \sigma 2)\right)^2$

$er1 \leftarrow er_0$

$er2 \leftarrow er_1$

$er3 \leftarrow er_2$

$Misfit \leftarrow \frac{er1 + er2 + er3}{n}$

$Model_{i+1,0} \leftarrow i + 1$

$Model_{i+1,1} \leftarrow h1$

$Model_{i+1,2} \leftarrow \sigma 1$

$Model_{i+1,3} \leftarrow \sigma 2$

$$
\begin{array}{l}
\left|\begin{array}{l}
\blacksquare \\
\mathrm{Model}_{i+1,4} \leftarrow \mathrm{Misfit} \\
\mathrm{sum} \leftarrow \mathrm{sum} + 1 \\
\mathrm{Model}_{i+1,1} \leftarrow \mathrm{Model}_{i,1} \ \text{ if } \ \mathrm{Model}_{i+1,4} > \mathrm{Model}_{i,4} \\
\mathrm{Model}_{i+1,2} \leftarrow \mathrm{Model}_{i,2} \ \text{ if } \ \mathrm{Model}_{i+1,4} > \mathrm{Model}_{i,4} \\
\mathrm{Model}_{i+1,3} \leftarrow \mathrm{Model}_{i,3} \ \text{ if } \ \mathrm{Model}_{i+1,4} > \mathrm{Model}_{i,4} \\
\mathrm{Model}_{i+1,4} \leftarrow \mathrm{Model}_{i,4} \ \text{ if } \ \mathrm{Model}_{i+1,4} > \mathrm{Model}_{i,4} \\
\text{break if } \mathrm{Model}_{i+1,4} < 1 \cdot 10^{-14}
\end{array}\right| \\
\mathrm{Model}
\end{array}
$$

Par(r,stations) outputs a matrix with the different columns containing inversion results for diffirent parameters The first row contains the starting model while the second row contains the inversion results after the first iteration etc.. The first column contains the number of iterations. The inversion process stops when the Misfit < 1*10E-14 (parts of primary field)^2 or when iterations = r. The Misfit after each iteration can be seen in the last column.

$$
\mathrm{Par}(5,0) = \begin{pmatrix}
0 & 5 & 0.05 & 5 \times 10^{-3} & 3.690266 \times 10^{-8} \\
1 & 7.016921 & 0.023415 & 6.094996 \times 10^{-3} & 1.998194 \times 10^{-9} \\
2 & 7.445276 & 0.022065 & 3.622749 \times 10^{-3} & 1.590968 \times 10^{-10} \\
3 & 8.162391 & 0.021468 & 2.772723 \times 10^{-3} & 6.459101 \times 10^{-11} \\
4 & 9.12883 & 0.02062 & 1.951741 \times 10^{-3} & 3.062416 \times 10^{-11} \\
5 & 9.657995 & 0.02023 & 1.395182 \times 10^{-3} & 7.288085 \times 10^{-12} \\
6 & 9.908012 & 0.020058 & 1.110837 \times 10^{-3} & 7.567034 \times 10^{-13}
\end{pmatrix}
$$